DOI: 10.1002/anie.201301487

Redox-Active Ligands

Complexes with Nitrogen-Centered Radical Ligands: Classification, Spectroscopic Features, Reactivity, and Catalytic Applications

*Alma I. Olivos Suarez, Volodymyr Lyaskovskyy, Joost N. H. Reek, Jarl Ivar van der Vlugt, and Bas de Bruin**

Keywords:
aminyls · nitrenes · imidyls · nitridyls · redox-active ligands

Dedicated to Prof. Karl Wieghardt

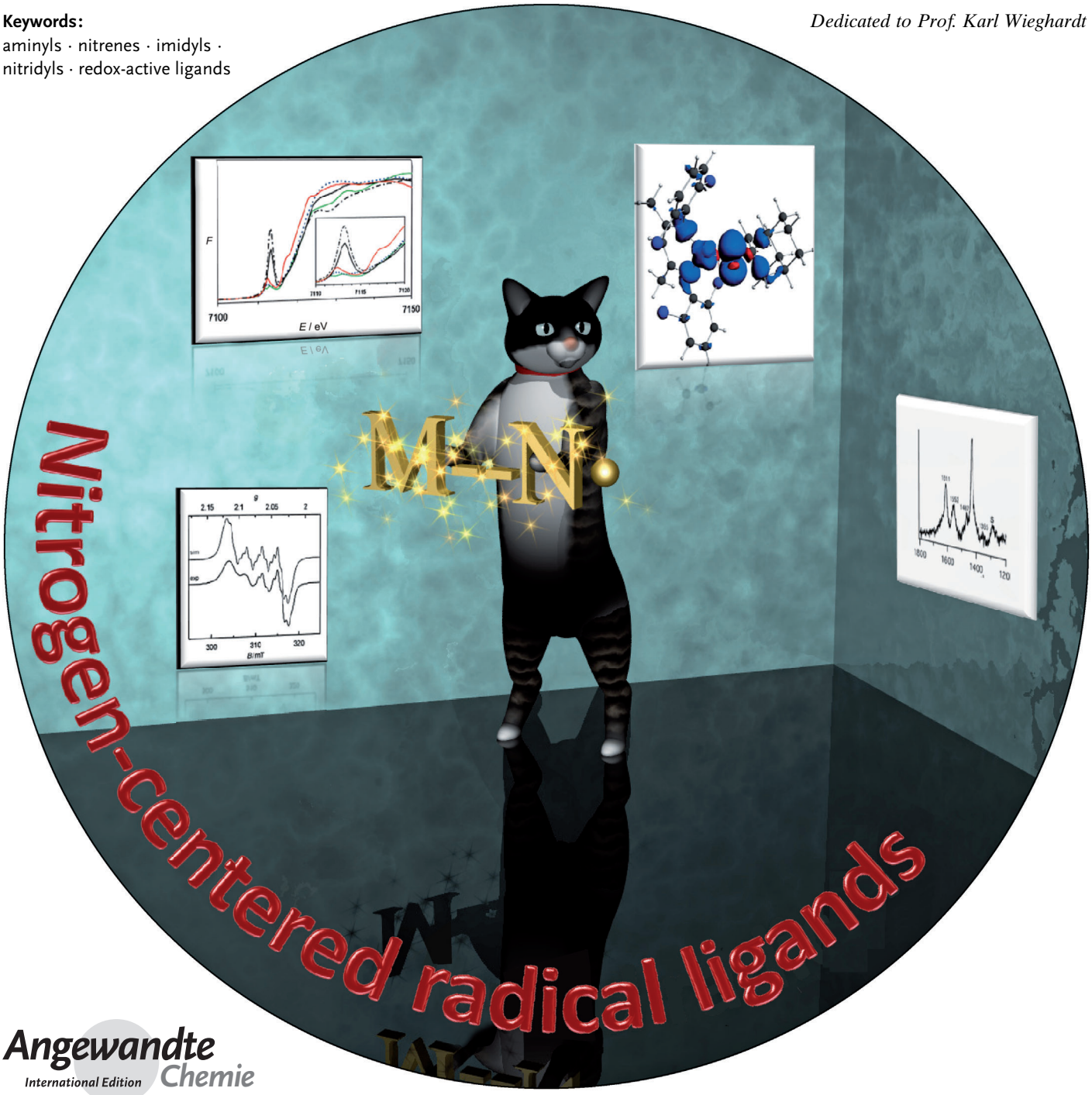

Angewandte International Edition Chemie

The electronic structure, spectroscopic features, and (catalytic) reactivity of complexes with nitrogen-centered radical ligands are described. Complexes with aminyl ([M(·NR$_2$)]), nitrene/imidyl ([M(·NR)]), and nitridyl radical ligands ([M(·N)]) are detectable and sometimes even isolable species, and despite their radical nature frequently reveal selective reactivity patterns towards a variety of organic substrates. A classification system for complexes with nitrogen-centered radical ligands based on their electronic structure leads to their description as one-electron-reduced Fischer-type systems, one-electron-oxidized Schrock-type systems, or systems with a (nearly) covalent M–N π bond. Experimental data relevant for the assignment of the radical locus (i.e. metal or ligand) are discussed, and the application of complexes with nitrogen-centered radical ligands in the (catalytic) syntheses of nitrogen-containing organic molecules such as aziridines and amines is demonstrated with recent examples. This Review should contribute to a better understanding of the (catalytic) reactivity of nitrogen-centered radical ligands and the role they play in tuning the reactivity of coordination compounds.

From the Contents

1. Introduction

Investigations into the ligand-centered reactivity of transition-metal complexes with so-called "cooperative" and "redox-active" ligands is currently among the "hot topics" of coordination chemistry and homogeneous catalysis.[1] In particular, ligands that can assist in catalytic transformations by storing and releasing electrons during catalytic turnover have attracted a lot of interest over the past years.[2] Such "redox non-innocent" (redox-active) behavior of ligands has received further attention because of the related ligand-centered redox processes observed in several metalloenzymatic reactions,[2,3] which in fact initiated the study of redox-active ligands in the first place. Meanwhile it has resulted in the development of a number of efficient and practically useful "bio-inspired" catalytic transformations.[4]

In the context of the above topics, the nitrogen-centered redox activity of amido, imido/nitrene, and nitrido ligands is of particular significance and relevance. Redox-active nitrogen-based ligands have hitherto received far less attention than their oxygen-based analogues (some of which play a key role in catalytic and enzymatic oxidation reactions).[5] Furthermore, metal-coordinated nitrogen-centered radicals are generally more stable than free organic nitrogen-centered radicals, thus opening the door to potential catalytic applications.[6] Complexes bearing open-shell nitrogen donors are remarkable synthetic targets, and were elusive for a long time because their high reactivity/instability makes their isolation and sometimes even characterization challenging. Such species are proposed to be key intermediates in catalytic functionalization reactions of hydrocarbons, olefin aziridination, and related nitrene-transfer reactions, and are thought to be important in nitrogen-fixation processes. Nitrogen-centered ligand radicals are also of interest from a theoretical and spectroscopic point of view. Resolving their electronic structures is rarely trivial, and a combination of spectroscopic measurements and high-level computational studies are usually required to draw any conclusions about the locus of the unpaired electron(s) (ligand or metal) in such species. Finally, successful application of nitrogen-centered radical ligands in new catalytic transformations makes them valuable from a practical point of view. In this Review, we will discuss experimentally well-defined disubstituted (aminyl, Figure 1a),[7] monosubstituted (nitrene, Figure 1b), and unsubstituted (nitridyl, Figure 1c) nitrogen-centered radical ligands featured in transition-metal complexes. We will also discuss the reactivity and experimental characterization of these species to illustrate their practical relevance and we will highlight spectroscopic techniques available for the elucidation of their electronic structures. Ligand radicals based on highly delocalized (1e oxidized or reduced) π systems, such as *o*-phenylenediamines, iminosemiquinone, α-diimines, α-iminopyridines, pyridine-2,6-diimines, verdazyl, bipyridine, and terpyridine (and alike) are excluded from this Review (despite the fact that some of these systems bear significant spin density at their nitrogen atoms).[8]

We start by classifying the specific N-donor ligands in analogy with the nomenclature used for carbene species, that is, as Fischer- and Schrock-type complexes. Carbene complexes are typically classified as either Fischer-type species, with low-lying empty π*(M-L) antibonding orbitals (LUMOs), or Schrock-type systems, with high-lying filled

[*] A. I. O. Suarez, Dr. V. Lyaskovskyy, Prof. Dr. J. N. H. Reek, Dr. Ir. J. I. van der Vlugt, Prof. Dr. B. de Bruin
Homogeneous and Supramolecular Catalysis
van't Hoff Institute for Molecular Sciences (HIMS)
University of Amsterdam
Science Park 904, 1098 XH Amsterdam (The Netherlands)
E-mail: b.debruin@uva.nl

π(M-L) bonding orbitals (HOMOs). These different orbital arrangements explain the electrophilic reactivity of Fischer-type carbene complexes and the contrasting nucleophilic reactivity of Schrock-type carbenes.[9] While unconventional for nitrogen-based systems, an analogous Fischer/Schrock-type classification applies well and proves to be useful in the discussion of the electronic structure of the radical ligand complexes considered in this Review. Nitrogen-centered radical ligands (aminyl, imidyl, and nitridyl radicals; see Figure 1) can be generated by either one-electron (1e) reduction of nitrenium ions, nitrenes, or nitrenates (Figure 1, species on the left) or by 1e oxidation of azanide, imido, or nitrido precursors (Figure 1, species on the right). Similarly, the corresponding metal complexes are formally derived from (hypothetical) nitrenium, nitrene, or nitrenido complexes (1e reduction of Fischer-type species with low-lying metal d orbitals, Figure 2a) or from amido, imido, or nitrido complexes (1e-oxidation of Schrock-type species with low-lying nitrogen p orbitals, Figure 2b). These systems are stoichiometrically identical, but electronically distinct. In the 1e-reduced Fischer-type complexes, the nitrogen-based SOMO is predominantly an antibonding π* orbital constructed from a nitrogen p orbital and a transition-metal d orbital, whereas in the 1e-oxidized Schrock-type case it is a bonding π orbital. Covalent complexes (roughly equal contribution of the metal and nitrogen atomic orbitals to the SOMO) are also possible, and these represent the borderline between ligand radicals and their metalloradical congeners (Figure 2c).

Several techniques are available to distinguish between metal- and ligand-centered radicals, of which EPR spectroscopy is probably the most important one. Radical ligands frequently have spectroscopic features that resemble those of free organic radicals: rather sharp well-resolved EPR signals,

Volodymyr Lyaskovskyy (born 1981) studied chemistry at Kiev National Taras Shevchenko University (Ukraine). He completed his PhD at the University of Münster (Germany) under the supervision of Prof. Dr. E.-U. Würthwein in 2007, working on novel electrocyclic reactions. In 2008 he started postdoctoral research in the group of Prof. K. Lammertsma (VU Amsterdam, the Netherlands) working on the chemistry of phosphinidenes. He is currently a postdoctoral researcher at the University of Amsterdam in the group of Prof. B. de Bruin. His research focuses on the study of redox-active nitrogen ligands.

Alma I. Olivos Suarez, born in Mexico City in 1983, studied chemistry at the Universidad Nacional Autónoma de México. She obtained her MSc in 2008 in the field of the adsorption of metals in environmentally relevant nanoparticles. In 2009 she started her PhD at the University of Amsterdam (The Netherlands) under the supervision of Prof. B. de Bruin in the field of homogeneous catalysis, focusing on metal-mediated carbene and nitrene transfer reactions.

Bas de Bruin (born 1971) completed his PhD at the RUN in Nijmegen (Prof. A. W. Gal, 1999). After postdoctoral research at the MPI für Bio-Anorganische Chemie in Mülheim (Prof. K. Wieghardt), he returned to the RUN as an assistant professor. In 2005 he moved to the University of Amsterdam, where he was promoted to associate professor in 2008 and to full professor in 2013. His research focuses on radical organometallic chemistry, EPR spectroscopy, olefin oxygenation, polymer synthesis, mechanistic studies, and computational catalysis, particularly on the development of new (bio-inspired) catalytic transformations.

Jarl Ivar van der Vlugt (born 1975) completed his PhD at the TU/e in Eindhoven (Prof. Vogt, 2003). After postdoctoral research in the USA (Univ. Illinois at Urbana-Champaign; Prof Rauchfuss) and Germany (Göttingen; Prof. Meyer) he became assistant professor at the University of Amsterdam (The Netherlands) in 2008. His scientific interests are in the functionalization of small molecules, hydroamination, bio-inorganic chemistry, catalysis for green energy applications, and ligand design.

Joost Reek (born 1967) did his PhD in Nijmegen (Prof. Nolte). After a postdoctoral fellowship in Sydney Australia with Prof. Crossley, he joined the group of Prof. van Leeuwen at the University of Amsterdam as an assistant professor (1998), with research activities focusing on transition-metal catalysis. In 2006 he became full professor. His research focuses on transition-metal catalysis, supramolecular catalysis, and catalysis for green energy applications. He founded a spin-off company (InCatT) to explore the commercial potential of supramolecular strategies for combinatorial approaches in catalysis.

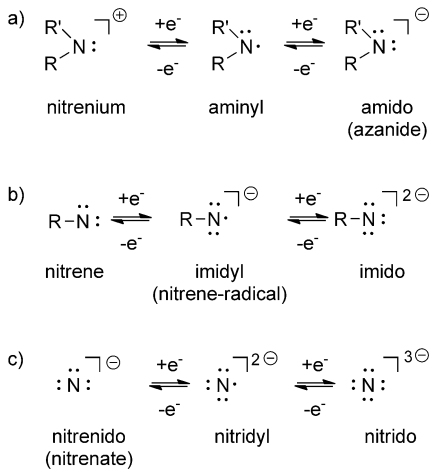

Figure 1. Lewis structures and nomenclature of a) disubstituted, b) monosubstituted, and c) unsubstituted nitrogen ligands.

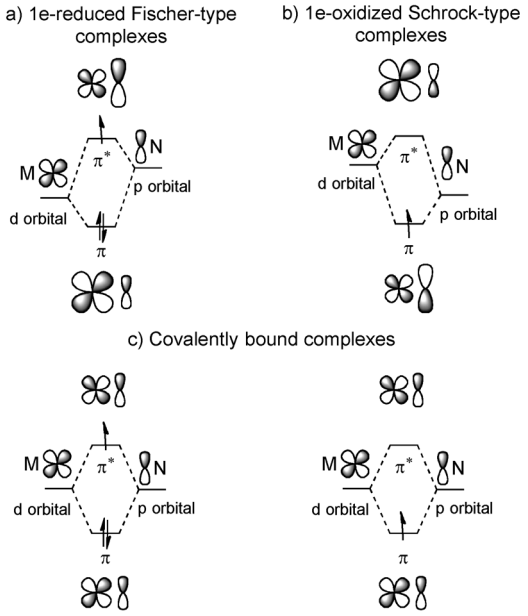

Figure 2. MO diagrams of open-shell nitrogen-centered radical ligands: a) 1e-reduced Fischer-type, b) 1e-oxidized Schrock-type, c) covalent complexes.

detectable at RT, and showing well-resolved ligand (super)-hyperfine coupling close to the *g*-value of the free electron ($g_e = 2.0023$). An illustrative example of an isotropic (solution-phase) EPR spectrum belonging to a ligand-centered radical complex is shown in Figure 3a.[10] Such species most often also reveal (nearly) isotropic signals, with small deviations from g_e, in frozen solutions. Metal-centered radical complexes, on the other hand, generally reveal much broader spectra as a result of rapid electron-spin relaxation effects. For this reason they are typically recorded at low temperature (e.g. frozen solutions < 70 K) and they tend to lead to anisotropic spectra. An example is shown in Figure 3b. Metalloradical complexes are typically (but not always!) associated with much larger *g*-anisotropies and larger deviations from g_e than radical ligand complexes.[10] Metal and

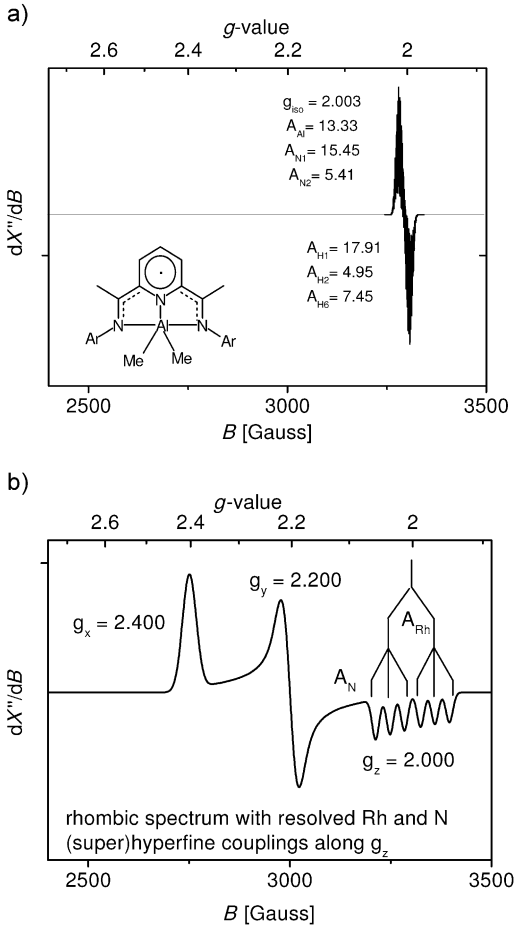

Figure 3. Illustrative examples of the EPR spectra of a) ligand- and b) metal-centered radical complexes.

ligand (super)hyperfine couplings can both be resolved, and are often of similar magnitude. Similarly, radical ligands can sometimes reveal rather large hyperfine couplings with the metal to which they bind. Hence, simply inspecting the *g*-values and magnitudes of (super)hyperfine interactions is not always enough to discriminate between metal- or ligand-centered radicals, and in many cases a more detailed analysis is necessary to draw solid conclusions (for a more detailed discussion, see Ref. [10]). Furthermore, interpretation of EPR spectra of $S > 1/2$ systems is generally much less straightforward. For this reason correlations between the experimental and (DFT) calculated EPR spectra are often very useful.

Mössbauer and X-ray absorption spectroscopy (XAS) are also very informative, since they are indicative of the electronic structure and oxidation state of the metal to which the redox-active ligand binds, and hence these techniques provide important, but indirect, information about the electronic structure of the whole complex. Quantum-chemical calculations (in particular population analysis of the spin density) are also extremely useful, especially considering the generally high reactivity of transient radical ligand species, which often complicates their characterization. A typical example of the spin-density plot of the radical ligand complex is shown in Figure 4. Here, most of the spin density is located

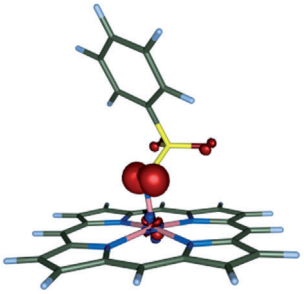

Figure 4. Spin density plot of a typical ligand-centered radical complex.

on the ligand (mainly on the nitrogen atom) and involvement of the metal in the delocalization of the unpaired electron is almost negligible.

2. Aminyl Radical Complexes

The first example of an experimentally unambiguously[11] detected redox-active aminyl radical complex was reported by Wieghardt and co-workers.[12] The Co^{III} complex $\mathbf{1}^{+}$ bearing an anilido (i.e. aryl amido) ligand was electrochemically oxidized, thus producing the dicationic species $\mathbf{1}^{2+}$ (Scheme 1). The X-band EPR spectrum (298 K) of $\mathbf{1}^{2+}$

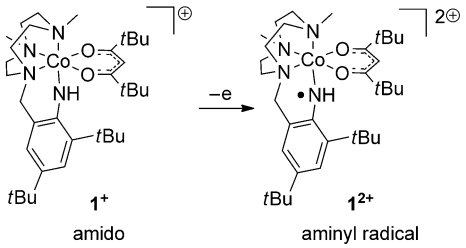

Scheme 1. Electrochemical oxidation of amido complex $\mathbf{1}^{+}$ to the Co^{III}-aminyl radical complex $\mathbf{1}^{2+}$.[12]

shows an isotropic signal typical for a ligand-centered radical complex, with a *g*-value of 2.0023 and strong hyperfine couplings to the cobalt atom ($A^{Co}_{iso} = 34$ MHz), the *N*H(Ar) nitrogen atom ($A^{N}_{iso} = 24$ MHz), the hydrogen atom of the N*H*(Ar) moiety ($A^{H}_{iso} = 29$ MHz), and the benzylic CH_2 hydrogen atoms ($A^{H}_{iso} = 26$ MHz). These values are remarkably similar to the ones reported for free ArHN· radicals, and thus point to an electronic structure that is best described as a ligand-centered aminyl radical complex.

The research group of Wieghardt further reported the related triazacyclononane manganese(IV) complex $\mathbf{2}^{+}$ with three anilido substituents. Cyclic voltammetry shows the complex to undergo three reversible electrochemical oxidation processes, which correspond to the formation of stable di- ($\mathbf{2}^{2+}$), tri- ($\mathbf{2}^{3+}$), and tetracationic ($\mathbf{2}^{4+}$) complexes, at least on the timescale of these measurements (Scheme 2). The three redox processes were interpreted as ligand-centered oxidations, and the oxidized species were all Mn^{IV} complexes, bearing one ($\mathbf{2}^{2+}$), two ($\mathbf{2}^{3+}$), or three ($\mathbf{2}^{4+}$) aminyl radical

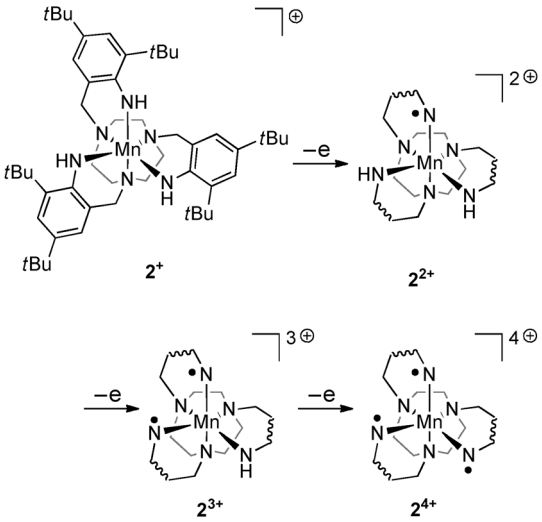

Scheme 2. Successive ligand-centered electrochemical oxidation processes with the manganese(IV) complexes $\mathbf{2}^{n+}$.[12]

ligands. The X-band EPR spectrum (10 K) of the dicationic species $\mathbf{2}^{2+}$ shows a signal at approximately $g = 4$. Assignment of the electronic structure of $\mathbf{2}^{2+}$ as either a triplet ($S = 1$) or quintet ($S = 2$) system is impossible solely on the basis of this EPR spectrum. However, a strong antiferromagnetic coupling is observed between the metal and the ligand radical in the analogous $[Cr^{III}(L^{\cdot})]^{+}$ complex, and thus a similar antiferromagnetic coupling between Mn^{IV} ($S_{Mn} = +3/2$) and the aminyl radical ligand ($S = -1/2$) is expected, which would lead to a triplet ($S = 1$) electronic structure for $\mathbf{2}^{2+}$.

The electronic structure of the tricationic species $\mathbf{2}^{3+}$ was elucidated as an $S = 1/2$ system. The EPR spectrum (10 K) of $\mathbf{2}^{3+}$ ($g_{iso} = 1.965$) shows clearly resolved hyperfine coupling with the metal center ($A^{Mn}_{iso} = 206$ MHz). The overall $S = 1/2$ electronic structure again arises from antiferromagnetic coupling between the three unpaired electrons on Mn^{IV} ($S_{Mn} = +3/2$) and the two ligand-centered radicals ($S_N = -1/2$ each). In agreement with the aforementioned strong M-L antiferromagnetic couplings, the tetracation $\mathbf{2}^{4+}$ is EPR silent. Unfortunately, the authors did not report any supporting computational studies, which currently prevent us from classifying these compounds as Fischer- or Schrock-type systems.

Grützmacher and co-workers were the first to report a stable and isolable aminyl radical transition-metal complex.[13] Deprotonation of Rh^{I} complex **3** followed by oxidation with ferrocenium hexafluorophosphate ($Fc^{+}PF_6^{-}$) leads to species **4**, which has been isolated and thoroughly characterized by EPR spectroscopy, X-ray diffraction, and DFT calculations (Scheme 3). The Q-band EPR spectrum (15 K) of **4** shows a rather small anisotropy of the *g*-tensor ($g_1 = 2.0822$, $g_2 = 2.0467$, $g_3 = 2.0247$), which indicates that spin–orbit interaction in **4** is much weaker than expected for a Rh^{II} center.[14] Pulse EPR techniques (Davies-ENDOR and HYSCORE) allowed a relatively large isotropic hyperfine coupling constant of the nitrogen atom of the aminyl radical ligand ($A^{N}_{iso} = 45$ MHz) to be detected, which was comparable to those observed for short-lived free dialkylaminyl

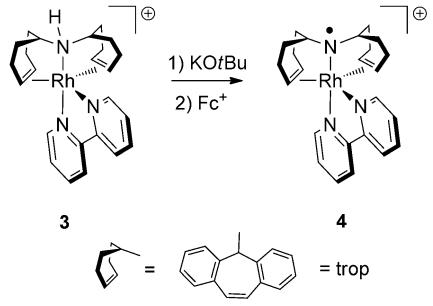

Scheme 3. Formation of stable, isolable Rh^{I}-aminyl radical complex **4**.[13]

radicals. DFT calculations further corroborate the redox-active properties of the *trop* ligand in **4**; ca. 54% of the total spin density is localized on the aminyl radical moiety and ca. 30% on the metal atom. The SOMO predominantly reflects the Rh-N π^* interaction (see Figure 2, 1e-reduced Fischer-type with a rather strong covalency).

As most of the spin density in the 18e complex **4** is located at the aminyl radical ligand, it can be expected to undergo ligand-centered radical-type reactivity. This is indeed observed, as **4** reacts quantitatively with hydrogen atom donors such as Bu_3SnH and PhSH. Complex **4** is not reactive enough towards PhOH, Ph_3SiH, or R_3CH. This result can be attributed to the higher E–H bond dissociation energies in these reagents. The iridium analogue of **4**, bearing a terpyridine instead of the bipyridine ligand, has a similar electronic structure, but with somewhat enhanced reactivity towards hydrogen atom donors as well as not fully understood intrinsic instability.[15]

A few related examples were obtained by deprotonation and oxidation of the 16e *trop* complexes **5** (Scheme 4).[16] The

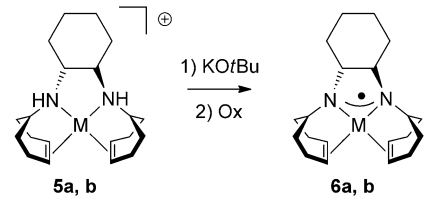

Scheme 4. Formation of delocalized aminyl radicals **6**.[16]

thus obtained open-shell species reveal higher reactivity than **4** towards solvent, which prevented characterization of the proposed radical species **6** by X-ray structure analysis. The reported EPR data of the rhodium complex were assigned to species **6a**. The spin population estimated from the experimental hyperfine constants amount to about 56% of the spin density in **6a** spread over the two nitrogen atoms. The complex is, therefore, described as a delocalized aminyl radical complex (calculated spin density per "aminyl nitrogen atom" 28%) with a considerable degree of covalency (41% spin density on Rh). The EPR spectrum of **6a** shows *g*-values close to 2, with a small anisotropy ($g_1 = 2.005$, $g_2 = 1.992$, $g_3 = 1.991$) and rather large hyperfine coupling with the nitrogen atoms ($A^{N}_{iso} = 11.1$, $A^{Rh}_{iso} = -0.7$ MHz). The Ir analogue **6b** is rather unstable, but EPR (X-band, HYSCORE, ENDOR) spectra could be obtained. The X-band EPR (20 K) spectrum with *g*-values close to 2 ($g_1 = 1.974$, $g_2 = 1.993$, $g_3 = 2.028$) again suggests that the unpaired electron is delocalized over the ligand, with only a minor contribution from the metal.

The aminyl radical species **6** are of interest from a reactivity point of view. Similar to **4**, they react with hydrogen atom donors such as stannanes, thiols, and silanes. Iridium complex **6b** is also postulated to be a key intermediate in the catalytic oxidation of alcohols to aldehydes in the presence of *t*BuOK (Scheme 5).[16c] The proposed mechanism

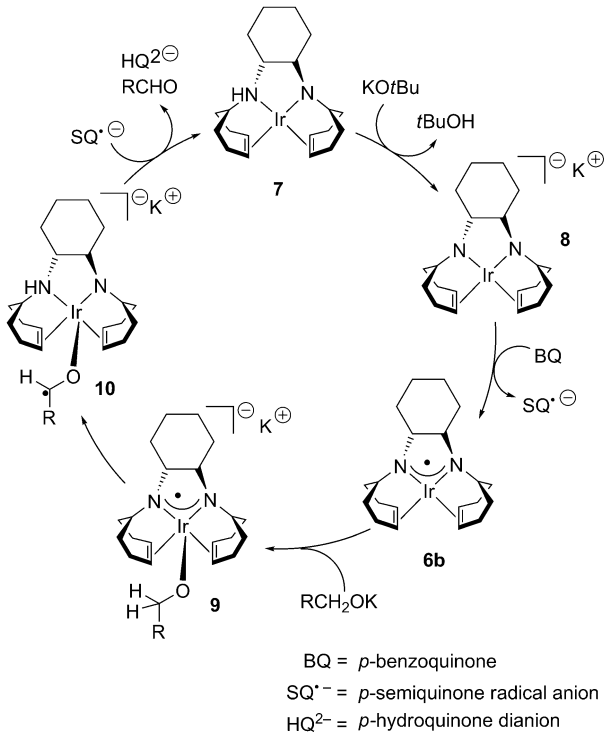

Scheme 5. Aminyl radical ligands in the catalytic oxidation of alcohols.[16c]

resembles the catalytic cycle of the enzymatic oxidation of galactose mediated by galactose oxidase.[17] The reaction starts by double deprotonation of the catalyst precursor **5b** to give the monoanionic intermediate **8** (via **7**), which is then oxidized by *para*-benzoquinone (BQ) to produce **6b**. This complex coordinates the alcoholate substrate, thus forming intermediate **9**, which undergoes intramolecular hydrogen atom abstraction (HAA) from the coordinated alcoholate to the redox-active aminyl radical ligand. A subsequent 1e oxidation of complex **10** by semiquinone and elimination of the aldehyde product closes the catalytic cycle. The reaction can be carried out with 1–10 equivalents of the base (KO*t*Bu), 2 equivalents of oxidant (benzoquinone is most efficient, but oxygen can also be employed), and very low catalyst loadings of 0.01 mol%, which provides the corresponding aldehyde with a remarkably high TOF (60000–150000 h^{-1}).

Pincer ligands are commonly used as ancillary ligands in organometallic chemistry,[18] but they can also act as electron reservoirs by delocalizing excessive (or deficient) electron density.[2] Incorporation of an amido functionality into a pincer motif can be employed to stabilize complexes with aminyl radical ligands. As such, Mindiola, Szilagyi, and coworkers reported the synthesis of [(PNP)NiCl]OTf complex **12a**, which was obtained in 87% yield by oxidation of the neutral precursor **11a** with FcOTf (Scheme 6).[19] X-ray

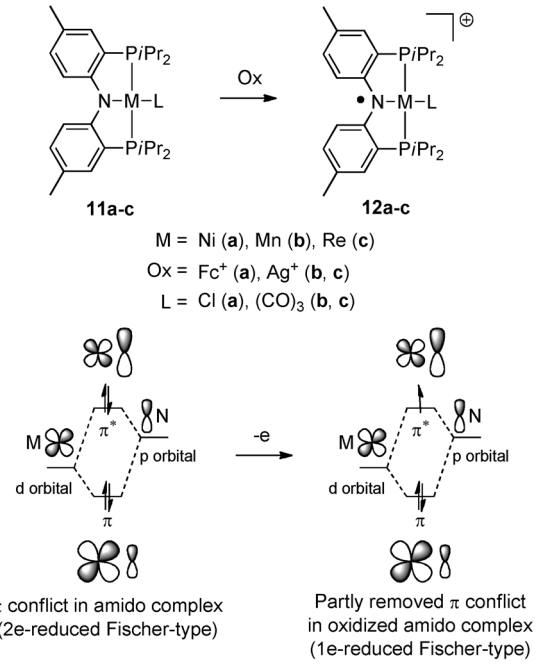

Scheme 6. Oxidation of electron-rich transition-metal amido complexes leading to aminyl radical complexes classified as "1e-reduced Fischer-type" species.[19,20]

crystallographic analysis of **12a** reveals a square-planar geometry around the Ni atom, very similar to neutral **11a**. Complexes **11a** and **12a** only differ slightly in their Ni-P-C_{Ar}-C_{Ar} dihedral angles. The X-band EPR spectrum of **12a** in solution (292 K) reveals well-resolved hyperfine couplings stemming from one N ($A^{N}_{iso} = 27$ MHz), two P, and six H atoms ($A^{P}_{iso} = 22$ MHz, $A^{H}_{iso} = 14$ MHz, $A^{H}_{iso} = 9$ MHz). The g_{iso}-value of 2.0238 further indicates an electronic structure that is best described as a ligand-centered aminyl radical complex (Ni^{III} species typically have g-values in the range 2.15–2.20). The Cl and P K-edge and Ni L_{III}-edge XAS spectra were also recorded. The latter proved highly informative for the electronic structure of **12a**. Only a slight change in the "$2p_{Ni}$→LUMO ($3d_{Ni}$)" excitation energy is observed upon oxidation of **11a** to **12a**, which indicates the presence of a Ni^{II} center in **12a** and, therefore, the redox process must be mainly ligand centered. In accordance with these experiments, DFT calculations reveal 69% spin density on the aminyl pincer moiety (32% on the nitrogen atom, 37% in the aromatic rings) and only 26% on the nickel atom. The HOMO of the amido precursor **11a** is dominated by a high-lying filled nitrogen p orbital in π conflict with a filled metal d orbital. Removal of one electron from the HOMO of **11a** partially reduces this π conflict and leads to a net π bond order of about 1/2 between the metal and the nitrogen atom of the aminyl radical. The unpaired electron resides predominantly in an antibonding π* Ni-N molecular orbital (SOMO), which is dominated by the contribution from the nitrogen p orbital (albeit with significant delocalization over the adjacent aryl rings). Species **12a** can, therefore, be classified as a "1e-reduced Fischer-type" species (Figure 2a; Scheme 6).

In a collaboration, the research groups of Nocera and Ozerov employed the same type of pincer ligand to generate Mn and Re aminyl complexes.[20] AgOTf was used as an oxidant in this case, which gave **12b** and **12c** in 98% and 86% yield, respectively (Scheme 6). Similar to the nickel couple **11a**/**12a**, the manganese and rhenium complexes undergo only a slight change in geometry on going from the neutral species **11b**,**c** to the cationic aminyl radicals **12b**,**c** (based on X-ray crystallography). Also the carbonyl C≡O stretch vibrations in the IR spectra reveal only a relatively small change upon oxidation of **11b**,**c** to **12b**,**c** ($\Delta\nu \approx 30$–40 cm^{-1}), thus pointing to electronic structures of **12b**,**c** that are best described as ligand-centered (not metal-centered) radicals. X-band EPR spectroscopic characterization of **12b**,**c** in a frozen solution (4 K) shows g-values close to 2.0 [$g_{iso} = 2.004$ (**12b**) and 2.013 (**12c**)]. The hyperfine couplings with the metal and N atom in **12b** are resolved at room temperature ($A^{Mn}_{iso} =$ 52 MHz; $A^{N}_{iso} = 25$ MHz), whereas **12c** revealed only metal-hyperfine coupling ($A^{Re}_{iso} = 169$ MHz, RT). DFT calculations confirmed the ligand-centered radical descriptions: For **12b**, only 14% spin density is localized on the Mn center and about 50% on the aminyl nitrogen atom; **12c** has about 7% spin density on the Re and 50% on the N atom. The electronic structure of **12b**,**c** is very similar to that of **12a** (1e-reduced Fischer-type, see Figure 2a, Scheme 6).

These species exhibit quite interesting radical-type reactivity. They proved unreactive toward PhSH and Et_3SiH, but reactions with hydrogen atom donors such as Bu_3SnH lead to the formation of the neutral species **11b**,**c**, likely by deprotonation of the intermediate hydrogen atom abstraction (HAA) products. The use of $Bu_3Sn(CH_2CH{=}CH_2)$ instead of Bu_3SnH leads to the allyl radical abstraction products **13b**,**c** (Scheme 7), which are stable under the reaction conditions and can be isolated. The observed attack at the aryl ring of the pincer ligand underlines the delocalized nature of the aminyl radical.

Application of a related PNP pincer ligand in copper complexes has been reported by Peters, Szilagyi, and co-

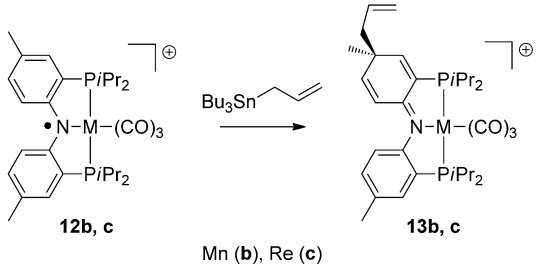

Scheme 7. Ligand-centered radical-type reactivity of **12b**,**c**.[20]

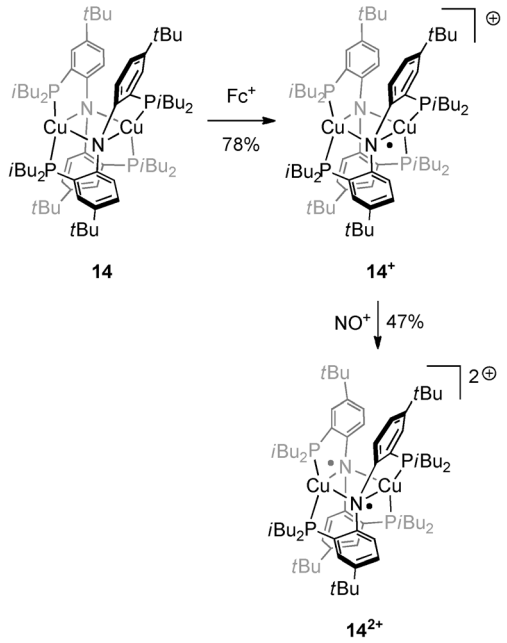

Scheme 8. Bridged aminyl radical ligands in Cu^{I} complexes.[21]

workers (Scheme 8).[21] In this case, however, a dinuclear dimeric structure **14** is formed with two bridging amido nitrogen atoms. The oxidation of **14** with 1 equivalent of a ferrocenium salt leads to monocationic Cu^{I} complex $\mathbf{14}^{+}$ (78% yield), in which one of the amido moieties of the pincer ligand is oxidized to an aminyl radical. The use of 2 equivalents of a nitrosonium salt as the oxidant leads to the oxidation of both ligands ($\mathbf{14}^{2+}$, 47% yield). The radical character of the pincer (aminyl) ligand(s) in $\mathbf{14}^{+}$ and $\mathbf{14}^{2+}$ means that the presence of *tert*-butyl groups is essential to prevent dimerization at the aryl rings (*para* position with respect to the aminyl nitrogen atoms).

Oxidation of **14** to $\mathbf{14}^{+}$ leads to shortening of the Cu-Cu distance by about 0.2 Å (from 2.72 to 2.53 Å, X-ray), whereas the second oxidation (to $\mathbf{14}^{2+}$) does not alter the Cu-Cu distance significantly ($d_{Cu\text{-}Cu}(\mathbf{14}^{2+}) = 2.53$ Å). The EPR spectrum of complex $\mathbf{14}^{+}$ features a broad signal without resolved hyperfine couplings and a rather small *g*-anisotropy ($g_1 = 1.987$, $g_2 = 2.025$, $g_3 = 2.098$). The EPR spectrum of $\mathbf{14}^{2+}$ is typical for an $S = 1$ system, with effective *g*-values at $g_1 = 1.998$ and $g_2 = 4.02$ (featureless).

Further evidence for the redox-active behavior of the ligand in $\mathbf{14}^{+}$ and $\mathbf{14}^{2+}$ was obtained from XAS spectroscopy. A negligible shift (< 0.5 eV) of the Cu K-edge inflection point on going from **14** to $\mathbf{14}^{+}$ indicates that the Cu centers have the same oxidation state in the two species (Cu^{I}). However, oxidation to $\mathbf{14}^{2+}$ leads to a somewhat larger shift of 1.7 eV in the Cu K-edge spectrum, which is attributed (based on a comparison with related species) to an asymmetric distortion of the $Cu_2(\mu\text{-}NR_2)_2$ core. The authors concluded from these data that $\mathbf{14}^{2+}$ is indeed a Cu^{I}-bis(aminyl) complex.

The electronic structure of triplet species $\mathbf{14}^{2+}$ was further investigated computationally through DFT calculations, and is in agreement with the experimental data. The two copper atoms carried only 35% of the total spin density, and most of the spin density (165%, two unpaired electrons corresponds to 200%) of $\mathbf{14}^{2+}$ is computed to be delocalized over the pincer ligands. Each of the two nitrogen atoms bears 77% spin density, which signifies rather delocalized ligand-centered radicals with a pronounced aminyl character. The strong covalency of the Cu–N bond in the cluster makes unambiguous assignment of the formal oxidation state in the monocationic compound $\mathbf{14}^{+}$ difficult.

The above-described aminyl radical complexes all contain chelating aminyl moieties. The first complex with a nonchelating aminyl ligand radical was reported by Peters, Szilagyi, and co-workers in 2009.[22] The anionic copper species **15a** was oxidized with a ferrocenium salt to yield neutral paramagnetic complex **16a** (25% yield; Scheme 9). The molecular struc-

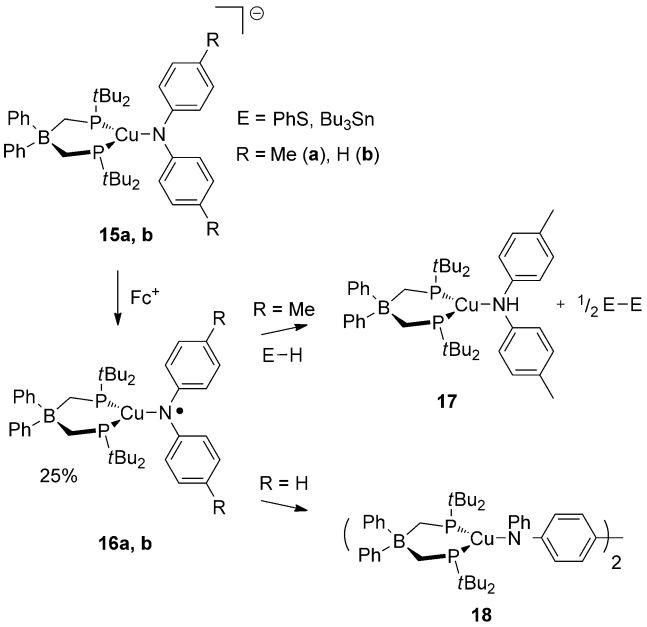

Scheme 9. Formation of aminyl radical **16** and its radical-type reactivity leading to hydrogen atom abstraction (R = Me) or *p*-phenyl dimerization (R = H).[22]

tures obtained by X-ray crystallography reveal a trigonal planar coordination geometry around the metal center for both species, with minor differences in the Cu–P bond lengths and P-Cu-P bond angles for **15a** and **16a**. However, shortening (ca. 0.1 Å) of the Cu–N bond is evident upon oxidation of **15a** to **16a**. This indicates (partial) removal of the π conflict between filled metal d orbitals and the completely filled nitrogen p orbitals (Fischer-type system) upon formation of the aminyl radical ligands (1e-reduced Fischer-type). The reported DFT calculations seem to be in agreement with this interpretation, although the picture is slightly blurred because of the somewhat strained bridging interactions and substantial delocalization over the ligand π system.

Cu K-edge XAS experiments show similar pre-edge and rising-edge energies for **15a** and **16a**, which indicates a similar "spectroscopic" oxidation state (d-electron configuration) of both species (i.e. Cu^{I}). Additionally, integration of the area under the pre-edge feature in the Cu L-edge XAS spectrum of

16a and comparison with the corresponding XAS area of $CuCl_2$ show that the redox-active molecular orbital in **16a** has only about 14% 3d-orbital character. These data correlate well with a ligand-centered oxidation on going from **15a** to **16a**.

Furthermore, the EPR spectrum of **16a** in frozen solution shows *g*-values close to 2.00 and substantial, well-resolved hyperfine couplings with the nitrogen atom (g_x, g_y, $g_z = 2.008$, 2.008, 2.030; A^N_x, A^N_y, $A^N_z = 24$, 100, 24 MHz). The DFT-calculated spin density on the nitrogen atom is 49%, and only 13% on the copper center (the residual spin density is delocalized over the tolyl moiety and P*t*Bu groups), which further supports **16a** having an aminyl radical ligand.

Consistent with its radical ligand character, complex **16a** demonstrates HAA reactivity towards hydrogen donors, such as thiophenol and tributyltin, and yields product **17**. Notably, if the tolyl group on the aminyl nitrogen moiety is substituted by a phenyl group (**15b**), oxidation by ferrocenium salts leads to a dimerization product **18**. Both reactions demonstrate the radical-type reactivity of aminyl radical species **16** (Scheme 9).

Another example of a nonchelating aminyl radical copper complex (although with a more covalent N–Cu bond) was reported by Warren and co-workers in 2010.[23] The target compound **20** can be prepared by reaction of lithium diphenylazanide ($LiNPh_2$) with the Cu^{II} precursor **19**, which gives "aminyl radical" complex **20** in 81% yield (Scheme 10).

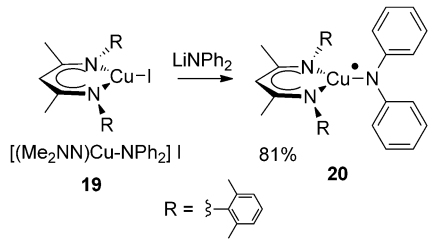

Scheme 10. Formation of aminyl radical complex **20** upon binding diphenylamide to Cu^{II} species **19**.[23]

Alternatively, **20** can be isolated (although in a lower yield of 31%) as a by-product of the reaction of diphenylnitrosamine (Ph_2NNO) with the Cu dimer [{$(Me_2NN)Cu$}$_2$]. X-ray crystallographic analysis reveals a shorter Cu-N distance (1.841 Å) in **20** than in **16a** (1.906 Å), and the anisotropy of the EPR spectrum (at 30 K) of **20** ($g_1 = 2.146$, $g_2 = 2.043$ and $g_3 = 2.018$; $A^{Cu}_1 = 298$ MHz) is much larger than observed for **16a**. The room-temperature EPR spectrum shows a relatively small hyperfine coupling with the aminyl nitrogen atom ($A^N_{iso} = 14$ MHz) and a large one with the Cu atom ($A^{Cu}_{iso} = 103$ MHz). DFT analysis also shows a stronger involvement of a copper d orbital in the SOMO, thus leading to similar spin densities on Cu (30%) and N (27%). The unpaired electron is further substantially delocalized over the two aryl rings. These data suggest that the Cu–N bond in **20** is rather covalent (Figure 2c). Nonetheless, complex **20** reacts as a ligand radical with other radicals such as NO, thereby leading to the formation of Ph_2NNO. The site of the initial NO attack (Cu or N) is currently unclear.

Many of the above examples describe "aminyl radical" complexes in which the aminyl moiety bears conjugated substituents capable of delocalizing the unpaired spin density of the aminyl radical. This typically results in substantial delocalization of the spin density over a larger ligand area, as described for most of the above examples.

The Rh^I-aminyl radical complex **4** described by Grützmacher and co-workers is a notable exception (Scheme 3). The rather strong covalency of the Rh–N bond in **4** nonetheless leads to substantial delocalization of the spin density over the metal and the ligand nitrogen atom.[13] Warren, Cundari, and co-workers recently reported another remarkable example wherein the aminyl moiety contains nonconjugated substituents.[24] Here, the reaction of dinuclear copper complex **21** with the lithium salt of 1-adamantylamine leads to aminyl radical complex **22** in 50–70% yield (Scheme 11). The X-band EPR (51 K) spectrum of **22** shows an anisotropic *g*-tensor ($g_1 = 2.133$, $g_2 = 2.036$, $g_3 = 2.031$). Also, the hyperfine tensors are anisotropic, with a large Cu hyperfine ($A^{Cu}_1 = 365$ MHz) and a substantial N_{aminyl} hyperfine splitting ($A^N_3 = 65$ MHz) evident. These data all point to a strong covalency of the Cu–N bond (Figure 2c), which was confirmed by DFT calculations. Spin-density calculations reveal 49% spin density on the aminyl nitrogen atom and 30% on the copper atom. The unpaired electron is located in a π*-Cu-N molecular orbital (1e-reduced Fischer-type with strong covalency; see Figure 2 and Scheme 6). Interestingly, the aminyl moiety in **22** participates in "nitrene" insertion reactions into the C–H bonds of ethylbenzene and indane to produce PhCH-(NHAd)Me and (1-indanyl)NHAd in 87% and 81% yield, respectively. These conversions were proposed to proceed through a binuclear mechanism, which reflects the importance of the [$R^1R^2N^{\bullet}$-Cu^I] resonance structure in the [R^1R^2N-Cu^{II}]↔[$R^1R^2N^{\bullet}$-Cu^I] resonance description of the nearly covalent Cu-N π interaction. HAA from the substrate (C–H bond) by the "aminyl radical" [$R^1R^2N^{\bullet}$-Cu^I] leads to formation of a Cu^I-amine species [R^1R^2N*H*-Cu^I] and an organic radical $R^{3\bullet}$. The latter reacts with another equivalent of the "aminyl radical" [$R^1R^2N^{\bullet}$-Cu^I] to form a Cu^I-amine product [$R^1R^2NR^3$-Cu^I] (see Scheme 11). The amine products readily dissociate from the Cu^I center.

Complex **22** could also be prepared directly from the free amine by using the *t*BuO complex **23** (Scheme 11). The latter was obtained by treating benzene-bridged dinuclear copper(I) complex **24** with *tert*-butylperoxide. Subsequent reaction of **23** with adamantylamine then yielded **22**. This method allows a remarkable direct catalytic amination of C–H bonds with amines,[24,25] and proceeds through the net "nitrene insertion" activity of **22**. In a typical procedure, the amine (1 equiv), *tert*-butylperoxide (1.2 equiv), the C–H substrate (10 equiv), and catalytic amounts of **24** (0.5 mol%) are heated at 90 °C, which gives the corresponding amines in high yields (Scheme 11). Not only substrates with activated C–H bonds such as indane and ethylbenzene can be employed, but also non-activated cyclohexane gives high yields of the corresponding amine product. Aliphatic amines such as Ad-NH_2, *c*-Hex-NH_2, $PhCH_2CH_2$-NH_2, and morpholine were evaluated

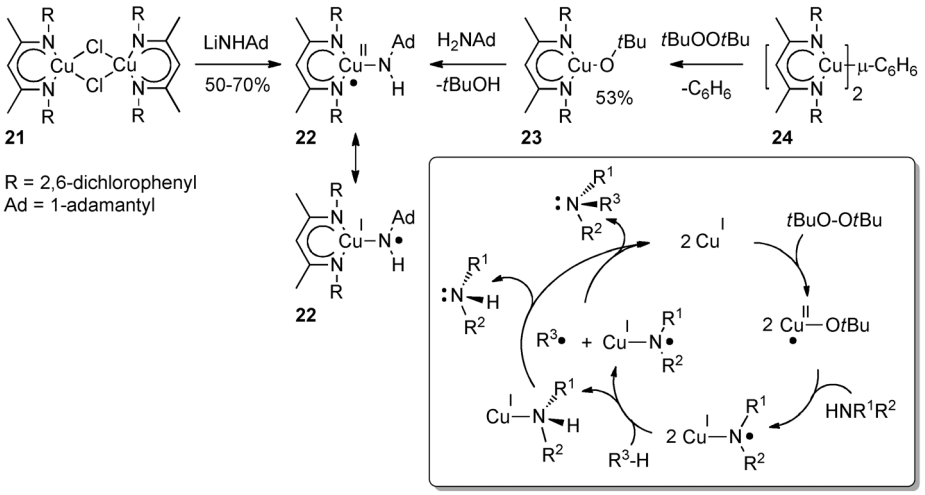

Scheme 11. "Nitrene transfer" activity of "aminyl radical" copper species **22** in the direct catalytic amination of C–H bonds with amines.[24]

as amines, and in all cases these led to C–H amination products in high yields. The scope of the reaction also includes aromatic amines,[25] but the formation of diazene decreases the yield, particularly with electron-rich anilines. Thus, optimum yields are obtained using anilines with electron-withdrawing groups (EWG) on the aromatic rings and low catalyst loadings to avoid dimerization. Remarkably, secondary amines can also be used, since the reaction proceeds via the aminyl complex $[R^1R^2N^{\bullet}\text{-}Cu^{I}]$ **22**, without formation of the nitrene precursor.

3. Nitrene Radical Complexes

Imido complexes are commonly proposed as intermediates in transition-metal-catalyzed nitrene transfer reactions. However, it was recognized (and proven) rather recently that in some cases such intermediates can have a considerable radical character on the imido(nitrene) nitrogen atom, which at least in part explains their reactivity.

Warren and co-workers were one of the first research groups to recognize the potential redox-active character of nitrene/imido ligands in a nickel complex.[26] The reported nickelimido complex **26** (Scheme 12) was prepared in 52% yield by treating the 2,4-lutidine-nickel complex **25** with 1-adamantylazide (AdN_3). X-ray crystallographic analysis of **26** revealed a slightly bent structure, with a Ni-*N*-C(Ad) angle of 164.5°. The frozen solution EPR (77 K) spectrum of **26** shows a rhombic pattern ($g_1 = 2.161$, $g_2 = 2.038$, $g_3 = 1.937$), where the central (g_2) signal is split into a triplet (1:1:1, $A = 63$ MHz) through nitrogen hyperfine coupling, thus supporting substantial participation of the nitrene/imido nitrogen atom ($I(^{15}N) = 1$) in the delocalization of the unpaired electron. However, the quite large *g*-anisotropy at low temperatures suggests considerable contribution of the metal to the SOMO. In accordance with the recorded EPR spectrum, DFT population analysis indicates that approximately 57% of the spin density is localized on the "nitrene" nitrogen atom. According to these calculations, the unpaired electron in **26** is located in an antibonding π* orbital, thus allowing the classification of **26** as a 1e-reduced Fischer-type nitrene complex (Figure 2a), although with a large covalent character of the M-N π bond. The "nitrene" moiety of **26** can be transferred to CO, PMe_3, and CN*t*Bu to form the corresponding AdN=X (**27**; X = Lewis basic molecule) organic products.[26] The reaction of **26** with the single-electron reducing agent cobaltocene unexpectedly produced $[Me_2NN]$Ni-N(Ad)-Cp-CoCp **28** as the product, further illustrating the radical character of **26**. The radical character of **26** is also reflected in its HAA reactivity towards 1,4-cyclohexadiene, which leads to the amido complex $[Me_2NN]$Ni-NHAd **29** and benzene.[26] The HAA reactivity was investigated with other benzylic C–H substrates in stoichiometric reactions. Capture of the generated alkyl radical $R^{2\bullet}$ through a rebound mechanism was demonstrated to lead to amino complex **31**. However, **26** has a similar affinity for the radical $R^{2\bullet}$ and leads to amido complex **30** (Scheme 12).[27] The nonselective C–H functionalization reactivity of **26** compared to **22** and its putative $\{[Cl_2NN]Cu]_2(\mu\text{-NAd})\}$ precursor is noteworthy. The somewhat enhanced selectivity of $R^{2\bullet}$ towards **26** compared to

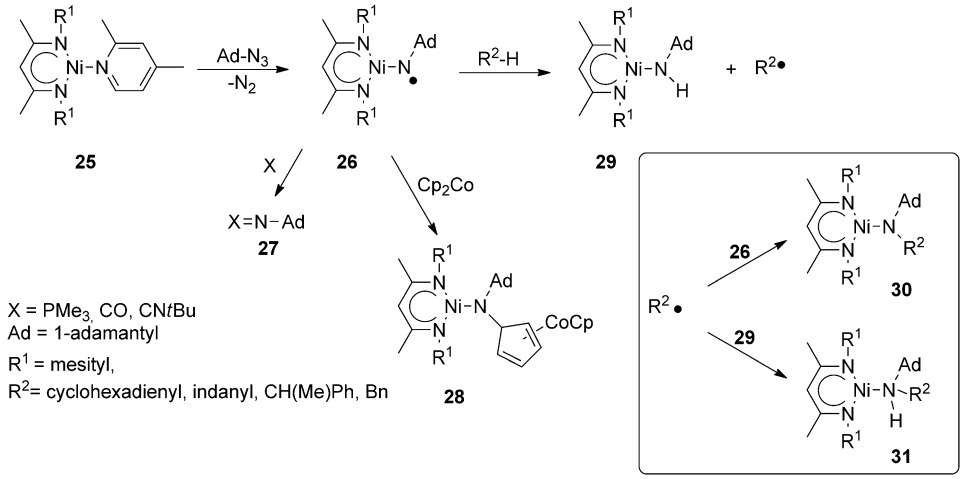

Scheme 12. Radical-type reactivity of "nitrene radical" complex **26**.[26] Cp = C_5H_5, Bn = benzyl.

{[Cl_2NN]Cu]$_2$(μ-NAd)} likely correlates with the imidyl character of **26**.

Another interesting nickel species that has been shown to participate in nitrene transfer reactions is the (dtbpe)Ni=NR (dtbpe = 1,2-*bis*(di-*tert*-butylphosphino)ethane) family of complexes reported by Hillhouse and co-workers.[28] These Ni^{II} imides **32** with a closed-shell configuration can undergo 1e chemical oxidation to afford their cationic analogues (**33a**) in 1,2-difluorobenzene (DFB; Scheme 13).[29] The ability of

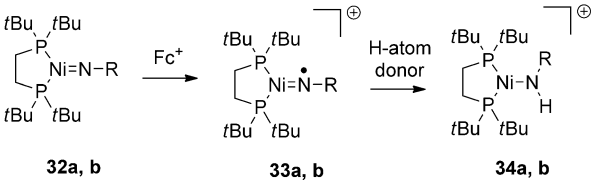

R = 1-adamantyl (**a**), 2,6-dimesitylphenyl (**b**).

Scheme 13. Synthesis of (dtbpe)Ni=nitrene radical complexes **33a**,**b** and their HAA reactivity.[28,29]

33a to abstract a hydrogen atom is remarkable, and the Ni^{II}-amide complex **34a** is obtained even in the presence of ethereal solvents. SQUID data for compound **33a** suggested a mixed spin state, and it was demonstrated that the doublet and quartet spin states of **33a** are involved in a temperature-dependent spin-crossover equilibrium (LS/HS = 1:4 at RT). Complex **33b** with a bulkier substituent on the imido moiety shows greater stability and does not reveal any spin crossover over a broad temperature range. The geometrical differences between complexes **33a** and **33b** (angle Ni-N-R is 164.2° for **33a** and 178.4° for **33b**) suggests that the aromatic ring in **33b** contributes to the delocalization of the electron density at the imido moiety, hence enlarging the Ni-N-R angle, which leads to enhanced orbital overlap. The reported EPR data of **33a** (broad isotropic line at ca. $g = 2.0$) and **33b** (overlapping patterns with features at ca. $g = 4$ and $g = 2.0$) did not allow the authors to distinguish between a metal- or ligand-centered radical, because of unresolved hyperfine couplings and because metal-centered Ni^{III} radicals have *g*-values in the range of 2.15 to 2.20. However, DFT calculations on simplified models reveal that the spin density is delocalized over the nitrogen and nickel atoms, with more than 50% spin density located at the nitrogen atom in both alkyl- and aryl-substituted species (69% for the alkyl-nitrene radical and 53% for the aryl-nitrene radical). Hence, the authors attribute the difference in reactivity of **33a** and **33b** to the radical character of the nitrogen atom. The theoretical model further suggests that the barrier for rotation around the Ni=NR bond is approximately 3 kcal mol^{-1} larger for the aryl-imido complex than the alkyl-imido species, which supports spin delocalization over the aryl ring in complex **33b**. In these DFT models the SOMO is located at the π*(d_{xz}-p_x) orbital, with the major nitrogen character in the alkyl-substituted complex pointing to a 1e-reduced imido complex (Fischer-type nitrene radical, Figure 2a). The aryl-substituted compound, however, has a more covalent Ni=NR π bond. Further characterization is needed to fully comprehend the electronic structure of these species.

Tanaka and co-workers prepared Ru-semiquinone-anilido complex **35** (Scheme 14), and a subsequent deprotonation with *t*BuOK gave the nitrene biradical species **36**.[30] The EPR

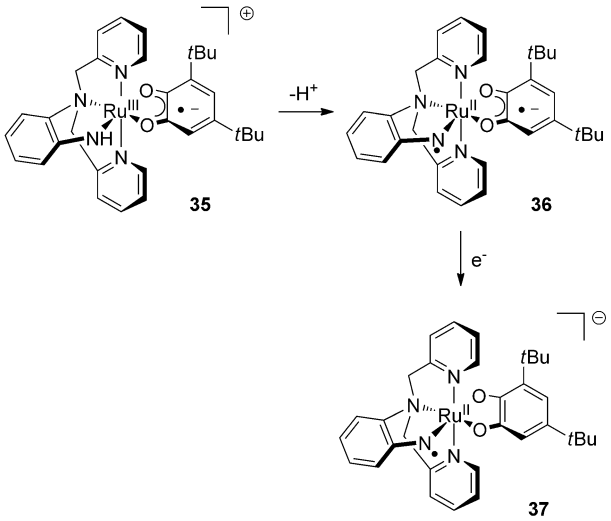

Scheme 14. "Nitrene radical" ruthenium complexes **36** and **37**.[30]

spectra of biradicals are generally not very illustrative of the locus of the unpaired electrons (and hence the redox-active behavior of the ligands). However, the fact that **36** is not EPR silent (two main transitions with *g*-values at ca. 2 and 4) can be taken as indirect evidence for the predominance of the [R•N-Ru^{II}] resonance structure over [RN=Ru^{III}], because Ru^{III}-semiquinone (SQ) species are expected to have strong antiferromangetic Ru^{III}-SQ couplings and are typically EPR silent. In accordance, DFT calculations show about 43% spin density on the nitrene nitrogen atom. Interestingly, compound **36** can be further reduced electrochemically to give the anionic species **37**. The latter also appears to be a ligand-centered radical with 64% spin density on the "nitrene" nitrogen atom and 31% on the ruthenium atom (DFT calculations). Complex **37** shows a rhombic *g*-tensor ($g_1 = 2.175$, $g_2 = 2.105$, $g_3 = 1.950$) in the EPR spectrum, with g_3 split into a triplet as a result of substantial hyperfine coupling with the nitrogen atom ($A^N = 224$ MHz). Again, a rather large *g*-anisotropy illustrates the considerable metal-radical character of the SOMO.

An open-shell system with several ligand-centered unpaired electrons was recently reported by Wieghardt, Lu, and co-workers. (Scheme 15).[31] Reaction of chromium biradical complex **38** (containing two 1e-reduced α-imine-pyridine ligands) with 1-adamantylazide leads to the formation of the neutral diamagnetic imido complex **39**, which in turn can be oxidized by two equivalents of ferrocenium salts to generate compound $\mathbf{39}^{2+}$ ($S = 1$). This complex contains two nonreduced α-imine-pyridine ligands and one 1e-oxidized "imido" ligand antiferromagnetically coupled to the three unpaired electrons on Cr^{III}. X-ray crystallographic analysis of $\mathbf{39}^{2+}$ shows a distorted trigonal-bipyramidal

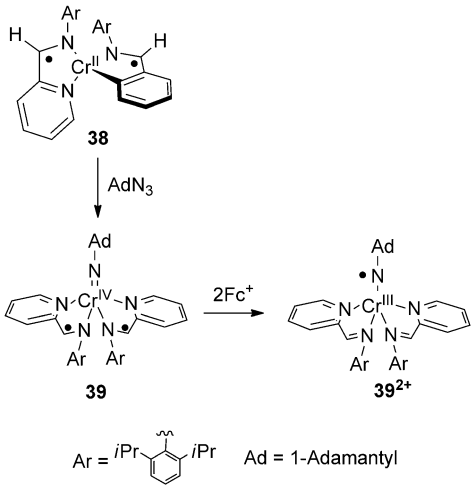

Scheme 15. Switching "redox activity" from the α-iminopyridine to the imido moiety upon oxidation.[31]

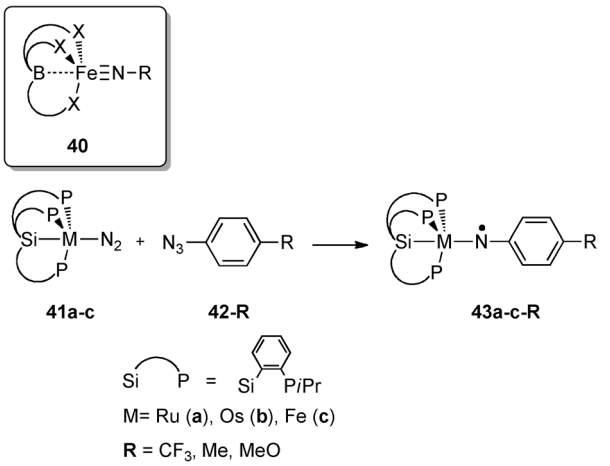

Scheme 16. "Delocalized nitrene radical ligands" reported by Peters and co-workers.[34–36]

geometry around the Cr atom, and a more linear Cr-N-C(Ad) fragment than in **39** [angle Cr-*N*-C(Ad) = 163.6° (**39**), 176.6° (**39**$^{2+}$)]. In this case, EPR spectroscopy did not allow the authors to distinguish between metal- and ligand-centered radicals. The authors, therefore, relied on Cr K-edge XAS, which indicated chromium in the oxidation state +III (Scheme 15). DFT calculations further corroborated the redox-active behavior of the nitrene ligand, and revealed 89% spin density on the "imido" nitrogen atom. Surprisingly, despite a considerable calculated spin density on the "imido" nitrogen atom in neutral **39** (78%, $S = 0$) and the monocationic **39**$^{+}$ (72%, $S = 1/2$), Cr K-edge XAS indicates the chromium in these complexes to be in oxidation state +IV (based on pre-edge and rising edge energies), which points to a "classical" imido AdN^{2-} fragment in **39** and **39**$^{+}$. It appears from the qualitative MO diagrams presented by the authors that the π*(M-NAd) MO is empty, which indeed indicates a 1e-oxidized imido (1e-oxidized Schrock-type) radical ligand (Figure 2b). However, a more detailed quantitative analysis of the MOs may be necessary to reach a final conclusion.

Multiple bonds between a metal center and an imido ligand can be achieved in the pseudotetrahedral environment of boranes **40** based on tris(phosphine)[32] or N-heterocyclic carbenes[33] (NHCs; Scheme 16). Substitution of the boron atom in **40** by silicon alters the geometry to trigonal bipyramidal or square pyramidal, which leads to a decrease in the M–N bond order and leads in some cases to nitrene radical complexes. In this way, Peters and co-workers prepared a series of complexes of the Group VIII elements with nitrene radical ligands. Thus, treatment of Ru or Os complexes **41a**,**b** with *para*-trifluoromethylphenylazide **42-CF$_3$** (Scheme 16, R = CF$_3$) gave rise to the formation of the nitrene radical complexes **43a-CF$_3$** (46% yield) and **43b-CF$_3$** (41% yield).[34] The room-temperature EPR spectra (low-temperature spectra were also recorded) revealed sharp patterns with g_{iso}-values close to 2.0 and large hyperfine constants with the nitrogen atom ($g_{iso} = 2.020$, $A^{N}_{iso} = 98$, $A^{P}_{iso} = 64$, $A^{Ru}_{iso} = 48$ MHz for **43a-CF$_3$**; $g_{iso} = 2.013$, $A^{N}_{iso} = 93$, $A^{P}_{iso} = 58$, $A^{Os}_{iso} = 155$ MHz for **43b-CF$_3$**). Species **43a-CF$_3$** and **43b-CF$_3$** were further characterized by X-ray structure analysis, which showed highly distorted trigonal bipyramidal geometries around the metal atoms (i.e. τ(**43a-CF$_3$**) = 0.54) and almost linear M-N-C bonds (ca. 170°). According to population analysis (DFT), about 25% of the spin density is located at the nitrogen atoms in **43a**,**b-CF$_3$**, while the total spin density on the ligands amounts to 54%. Hence, the radical is substantially delocalized over the metal and the NAr moiety. It is noteworthy that species **43a**,**b** also have some negative spin density on the nitrene substituent, which actually reduces the total ligand spin density.

Further studies showed that the nature of the organic group on the azide **42-R** has a big impact on the course of the reaction with **41a**.[35] Thus, the addition of *para*-methoxyphenylazide **42-OMe** (instead of **42-CF$_3$**) to **41a** yields *para*-(methoxy)azobenzene **45** and only a small amount of complex **43a-OMe** (Scheme 17). Remarkably, the formation of azoarene **45** does not proceed via complex **43a-OMe**, but via the free triplet aryl nitrene **44**, which either dimerizes or reacts with another molecule of aryl azide **42-OMe** to yield the azoarene. The nitrene species **43a-OMe** can, however, be prepared in 52% yield by reduction of cationic complex **46**

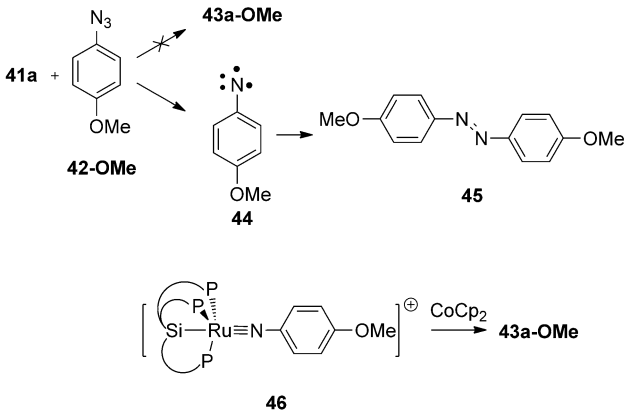

Scheme 17. Azo-arene formation via free triplet nitrene **44**, not via nitrene radical **43**.[35]

with cobaltocene (Scheme 17). Similar to **43a-CF$_3$**, complex **43a-OMe** can be described as a nitrene radical ligand species. The EPR spectrum of **43a-OMe** recorded at room temperature shows a three-line pattern with large nitrogen hyperfine couplings ($g_{iso} = 2.002$, $A^{N}_{iso} = 119$ MHz, $A^{Ru}_{iso} = 38$ MHz, $A^{P}_{iso} = 48$ MHz).

The analogous Fe complex **43c-Me** is rather unstable, and can be generated only by photolysis of the corresponding azide complex in frozen 2-(methyl)tetrahydrofuran glass at 77 K.[36] The EPR spectrum (77 K) of **43c-Me** has a somewhat anisotropic g-value (g_x, g_y, $g_z = 1.990$, 2.032, 2.098), but close to the value of 2.0, thus pointing to a strong ligand involvement in the SOMO. DFT calculations on a simplified model (low spin, ground state) showed about 16% spin density on the nitrogen atom and again a strong delocalization into the adjacent aryl moiety. Similar to complexes **43a,b-CF$_3$**, some negative spin density is found on the ligand, likely caused by spin polarization, which in turn results from antiferromagnetic coupling of the five unpaired electrons (total $S = 1/2$, 3 α and 2 β electrons). This reduces the total spin density on the "nitrene" moiety. DFT calculations also predicted a close-lying intermediate quartet spin state ($S = 3/2$) only about 2.8 kcal mol^{-1} higher in energy than the doublet ($S = 1/2$). The total nitrogen spin density in the quartet ($S = 3/2$) species is 82%. The unpaired electron of the lower-energy doublet ($S = 1/2$) species is located in the antibonding π^* orbital, and hence we classify this species as a 1e-reduced Fischer-type nitrene complex (Figure 2a).

The iron species **43c-Me** is too unstable to further study its reactivity directly. However, it is most likely a key intermediate in a number of reactions of species **41c** and azides **42**. The proposed intermediate **43c-Me** is capable of abstracting a hydrogen atom from 9,10-dihydroantracene to yield anthracene and Fe(NHTol)(SiP$^{iPr}_3$). Nitrene transfer to *tert*-butyl isocyanide (*t*BuNC) to give the corresponding carbodiimide (*t*BuN=C=NTol), azoarene (TolN=NTol), and the isonitrile complex Fe(SiP$^{iPr}_3$)(CN*t*Bu), is proposed to proceed via the same nitrene radical intermediate. In the absence of other reagents, the reaction of **41c** with tolylazide **42-Me** led to the formation of *para*-methylazobenzene (TolN=NTol). This reaction was also proposed to proceed via intermediate **43c-Me**.

Another interesting Fe-nitrene complex **48** (Scheme 18), was recently reported by Betley and co-workers. This species is more stable than **43c**, and hence could be characterized using X-ray crystallography.[37] Complex **48a** features a slightly elongated Fe–N bond (1.768 Å) compared to previously reported iron-imido complexes (1.66–1.73 Å), which suggests a decreased Fe–N bond order in **48a**. Mössbauer spectroscopy indicates an Fe^{III} d^5 configuration in **48a**, which likely correlates to transfer of a single electron from the metal to the ligand. DFT calculations reveal considerable positive as well as negative spin density on the "imido" nitrogen atom. Based on these data, species **48a** was identified as having six unpaired electrons. One electron, localized on the "imido" moiety ($S_N = -1/2$), is antiferromagnetically coupled with one of the other five unpaired electrons localized on the iron atom ($S_{Fe} = +5/2$), thus giving a total quintet ($S_{total} = 2$) spin multiplicity. This "imido" unpaired

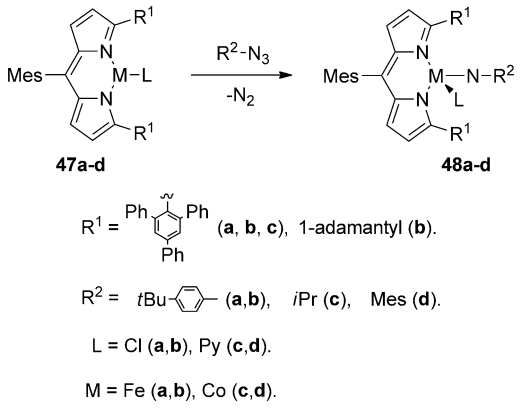

Scheme 18. "Half-porphyrin"-stabilized iron- and cobalt-nitrene radical complexes reported by Betley and co-workers.[37,38] Mes = mesityl.

electron is located in a predominantly π-bonding orbital between the metal and the "imido" nitrogen atom, thereby allowing the classification of this system as a Schrock-type 1e-oxidized imido ligand (Figure 2b). However, the picture is somewhat blurred because of substantial delocalization of spin density over the adjacent aryl ring.

The reactivity of **48a,b** further supports its nitrene radical nature. The nitrene moiety of **48a,b** can be transferred to organic substrates, and be used either for nitrene insertion into benzylic C–H bonds of toluene [to produce PhCH$_2$-NH(*p*-C$_6$H$_4$*t*Bu)] or in the aziridination of styrene [to produce Ph[CHCH$_2$]N(*p*-C$_6$H$_4$*t*Bu)]. The catalytic activity of **47** has also been briefly studied in the amination of toluene using adamantyl azide as a nitrene source. The best results were obtained with the 1-adamantyl-derived complex **47b**, which gives 95% yield of the (benzyl)(adamantyl)amine (PhCH$_2$-NHAd) at room temperature (TON = 6.7). Catalytic aziridination with **47b** is also possible, with styrene converted into the corresponding aziridine in 85% yield (neat styrene, RT, 20 equiv of AdN$_3$, TON = 17).

In line with the ability of the weak-field dipyrrin ligand to stabilize low coordination modes in **47a,b**, Betley and co-workers investigated the Co analogues **47d,c** and the parent imido species **48c,d**.[38] Despite most Co complexes displaying low-spin ground states, species **48c** has a partial population of the high-spin state ($S = 2$; 35% at RT) and undergo spin crossover from a singlet to a quintet state. This, however, is not the case with the aromatic analogue **48d**, which has an intermediate spin ($S = 1$). This is attributed to the conjugation of the nitrogen p orbital with the coplanar aromatic ring in **48d**, which changes the orbital energy diagram of the species. Complex **48c** undergoes imido/nitrene group transfer to phosphines, but no C–H bond activation of 1,4-cyclohexadiene or dihydroanthracene. Complex **48d**, however, is able to activate intramolecularly the C–H bond of the *ortho*-methyl group of the mesityl substituent on the imido ligand. On the basis of the available data the authors interpreted species **48c,d** as metal-centered radical complexes. Thus, a decrease in the HAA reactivity of **48**, when iron is substituted by cobalt, may point to the importance of ligand-centered radical complexes in these types of reactions.

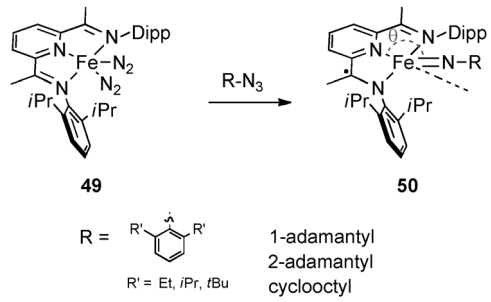

Scheme 19. Iron "imido" complexes stabilized by the redox-active PDI ligand.[39,40] Dipp = diisopropylphenyl.

Chirik and co-workers reported a series of Fe(nitrene) species **50** (Scheme 19), bearing the redox-active pyridine-2,6-diimine ligand (PDI). These complexes were prepared by treating bis(dinitrogen) complex **49** with the corresponding azide. The substituent on the nitrene nitrogen atom was found to have a big influence on the properties of the resulting species. Thus, in the case of R = Ar (Scheme 19), complexes **50-Ar** exhibit a relatively long Fe–$N_{nitrene}$ bond (1.705–1.717 Å) and a nonlinear N_{Py}-Fe-$N_{nitrene}$ structure ($\theta = 139$–$155°$, Scheme 19).[39] Those species are found (based on X-ray studies, Mössbauer spectroscopy, and SQUID magnetic studies) to have a triplet ($S = 1$) spin multiplicity, and thus best described as Fe^{III} intermediate spin-state ($S_{Fe} = +3/2$) systems antiferromagnetically coupled to a monoanionic PDI radical ligand ($S_{PDI} = -1/2$). As a consequence, the NAr moiety in these complexes behaves as a "classical" $[NAr]^{2-}$ imido fragment (**I**, Figure 5), with a rather covalent Fe–$N_{nitrene}$ bond and a 2-center-3e bond.

Quite a different picture is observed when the "nitrene" nitrogen atom carries an alkyl substituent.[40] Thus, species **50-Alk** with R = 1-adamantyl, cyclooctyl, or 2-adamantyl have relatively short Fe–$N_{nitrene}$ bonds of 1.65–1.66 Å and more linear N_{Py}-Fe-$N_{nitrene}$ angles ($\theta = 168$–$175°$) than the derivatives with R = Ar. These systems exhibit spin-crossover behavior. Complex **50-^{1}Ad**, in contrast to **50-Ar**, is found to be (almost) diamagnetic ($S = 0$) at room temperature (based on SQUID magnetic measurements), but spin-crossover to a triplet ($S = 1$) system occurs at elevated temperatures (ca. 8% of the $S = 1$ spin state between 50 and 200 K, with increased $S = 1/S = 0$ ratios at higher temperatures). In all cases, incomplete transitions toward the triplet spin state were observed at the temperatures studied. The 2-adamantyl derivative **50-^{2}Ad** shows similar behavior, with an $S = 1$ ground state at room temperature and spin crossover to $S = 0$ at lower temperatures.

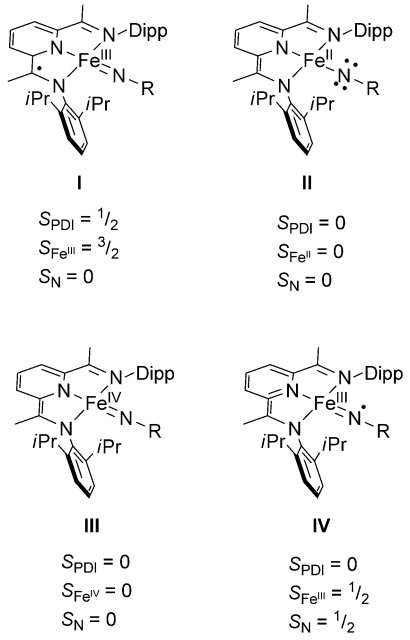

Figure 5. Possible electronic configurations of species **50**.[40]

Deducing and understanding the electronic structures of **50-Alk** species is not a trivial exercise. Both the iron center and the redox-active PDI ligand may adopt multiple redox states, and DFT calculations do not always reliably reproduce the relative energies of open-shell spin-crossover systems (with the commonly applied B3LYP functional frequently giving an artificial preference for the higher-spin states).[41] Based on the collected experimental data thus far, **50-^{1}Ad** ($S = 0$) can be interpreted either as a low-spin Fe^{II} or Fe^{IV} complex (**II** or **III**, Figure 5) or as an Fe^{III} species **IV** (Figure 5) with a low-spin Fe^{III} ($S_{Fe} = +1/2$) system antiferromagnetically coupled to a nitrene radical ligand ($S_N = -1/2$; Figure 5). An Fe^{III} species with an intermediate spin state ($S_{Fe} = +3/2$) could be excluded on the basis of Mössbauer spectroscopic data.

The electronic structure of **50-^{2}Ad** is perhaps even less clear and different from both **50-Ar** and **50-^{1}Ad**. Although it has the same total spin ($S = 1$) as **50-Ar**, the spectroscopic and geometrical differences between these two species did not allow the authors to classify the electronic structure of **50-^{2}Ad** as **I** (Figure 5). Three possible candidates for the electronic structure of **50-^{2}Ad** include: 1) an intermediate spin ($S_{Fe} = 1$) Fe^{II} (or Fe^{IV}) species with closed-shell PDI ($S_{PDI} = 0$) and nitrene ligands ($S_N = 0$); 2) **50-^{2}Ad** could contain a diamagnetic PDI fragment ($S_{PDI} = 0$) and a ferric (Fe^{III}) center ($S_{Fe} = +3/2$) antiferromagnetically coupled to a nitrene radical moiety ($S_N = -1/2$); 3) the electronic structure **IV** could also correlate with the experimental data; a low-spin Fe^{III} center ($S_{Fe} = +1/2$) ferromagnetically coupled with a nitrene radical moiety ($S_N = +1/2$).

The Fe–$N_{nitrene}$ bonds must display a considerable degree of covalency (closer to Figure 2c). The differences between the aryl- and alkyl-substituted nitrene species **50** most probably relate to steric factors, as the N-Ar substituent protrudes out of the Fe-PDI plane, because of its steric bulk, which decreases the Fe-$N_{nitrene}$ electronic overlap and consequently leads to a higher spin state on Fe. On the other hand, the N-Alk substituent is more in the Fe-PDI plane, thereby leading to a stronger orbital overlap between the Fe and $N_{nitrene}$, which further increases the covalency of the Fe–N bond and the nitrene field strength, which leads to a low-spin iron configuration.

Holland and co-workers reported an iron-imido complex stabilized by a β-diketiminate (nacnac) ligand.[42] This complex is rather redox-inert compared to the PDI ligand.

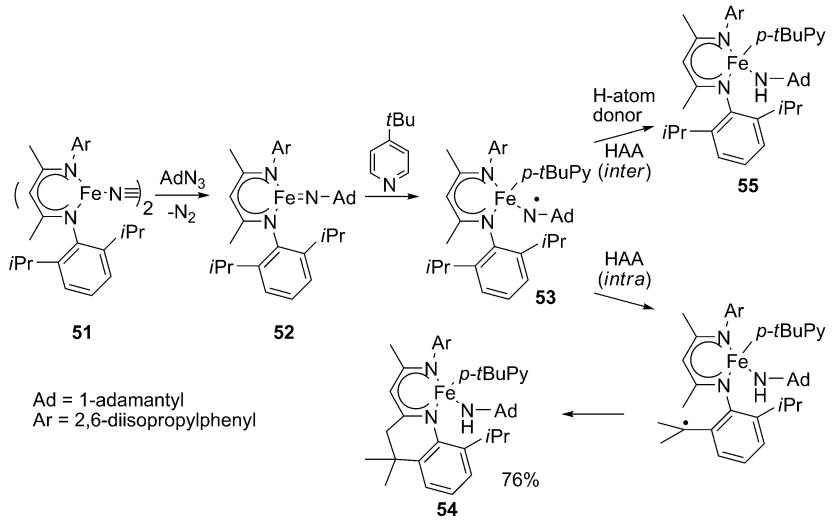

Scheme 20. Generation and HAA reactivity of iron "nitrene radical" **53**.[42]

Nitrene complex **52** was formed by treating dinitrogen complex **51** (Scheme 20) with 1-adamantyl azide. Species **52** was thoroughly characterized by X-ray, EPR, Fe K-edge XAS, EXAFS, and Mössbauer spectroscopy and supported by DFT calculations. According to the DFT data, about 23% of the spin density of **52** ($S = 3/2$) is localized on the "nitrene" nitrogen atom. The addition of several equivalents of *p*-(*tert*-butyl)pyridine changes the spin multiplicity of the species from quartet to sextet, thereby increasing the spin density on the "nitrene" nitrogen atom to 82% in **53**. Notably, the coordination of a pyridine ligand to **52** is essential to induce further reactivity, with **53** being capable of intra- and intermolecular (from 1,4-cyclohexadiene derivatives) HAA to produce **54** or **55**, respectively (Scheme 20). Based on the reported experimental and computational studies, the role of the coordinated pyridine ring in promoting the HAA activity of the complex **53** is explained by weakening of the Fe=NAd bond in **53**, and stabilization of the HAA products **54** and **55** through coordination of the pyridine ligand (thermodynamically driven reaction). The quartet ($S = 3/2$) and sextet ($S = 5/2$) electronic structures of **52** and **53** are interpreted as stemming from ferromagnetic coupling between the metal and ligand unpaired electrons.

A strategy to circumvent the unwanted intramolecular reactivity was to avoid the presence of weak C–H bonds near the imido moiety in **52**. Complex **57**, which features a β-diketiminato ligand with phenyl instead of isopropyl substituents, can be prepared from Fe^{I} precursor **56** (Scheme 21). Species **57** shows, similar to **52**, a rhombic X-band EPR (8 K) spectrum (**57a**: $g_{eff} = 7.11, 1.55, 1.26$; **57b**: 7.42, 1.05, 0.9), hence suggesting that **52** and **57** have similar electronic structures.[43] The phenyl moiety at the diketiminato ligand in **57** has a remarkable effect on the reactivity. Thus, although **52** is relatively unstable, complex **57** is stable for several days in benzene solution. More importantly, **57** shows much higher HAA reactivity (factor 145) than **52**, and the addition of pyridine was no longer necessary. Two factors contribute to such differences in reactivity. 1) A steric factor: rotation of the aromatic 2,4,6-triphenylphenyl substituent decreases the steric bulk on one side of the (N,N)Fe-NR plane of the compound, thus enabling an easier approach of the substrate. The metal center in **57**, however, is more crowded than in **52**, which lowers the affinity of **57** for pyridine. 2) The Fe-N-R angle of **57** is much smaller than in **52** (for R = Ad: 151° in **57**, and 170° in **52**) and the Fe–$N_{nitrene}$ bond longer (for R = Ad: $d_{Fe\text{-}N(nitrene)} = 1.70$ Å in **57** and 1.67 Å in **52**). This makes complex **57** closer in geometry to the transition state for HAA, which is predicted (QM/MM calculations) to have a Fe-$N_{nitrene}$ distance of 1.90 Å and a Fe=N-R angle of 140°.

The research groups of de Bruin and Zhang recently reported two Co^{III}(porphyrin) "nitrene radical" species

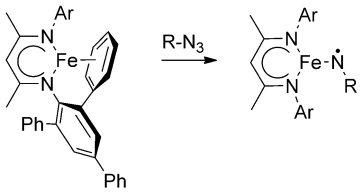

Scheme 21. A modified β-diketiminate ligand to stabilize nitrene radical compound **57**.[43]

59a,**b**,[44] which were generated by the reaction of the corresponding Co^{II}(porphyrin) species **58** with excess organic azide (Scheme 22). The radical character of the ligands of both derivatives of **59** was demonstrated by EPR spectroscopy and supported by DFT computational studies. The EPR spectra recorded in solution at room temperature showed sharp signals (ca. 100 Gauss signal width) with g_{iso}-values around 2.0, with hyperfine coupling with the cobalt (A^{Co}_{iso} = 25–27 MHz) and a single nitrogen atom (A^{N}_{iso} = 6–10 MHz; simulation parameters based on DFT-calculated values). According to Mulliken population analysis, about 60–90% (depending on substituent R^3) of the spin density of **59** is localized on the "nitrene" nitrogen atom (see Figure 4 for one example). The unpaired electron is located in a π*-antibonding Co-N MO and, therefore, **59** can be classified as a 1e-reduced Fischer-type nitrene complex (Figure 2a). In contrast to most of the above-mentioned examples, where the metal-nitrene complexes participate only in stoichiometric reactions, nitrene radical species **59** are key intermediates in practically useful catalytic C–H bond amination and olefin aziridination processes (Scheme 22).[4b,44b,45]

Interestingly, catalytic reactions with the sterically more encumbered cobalt(II)-porphyrin **58b**, bearing hydrogen-

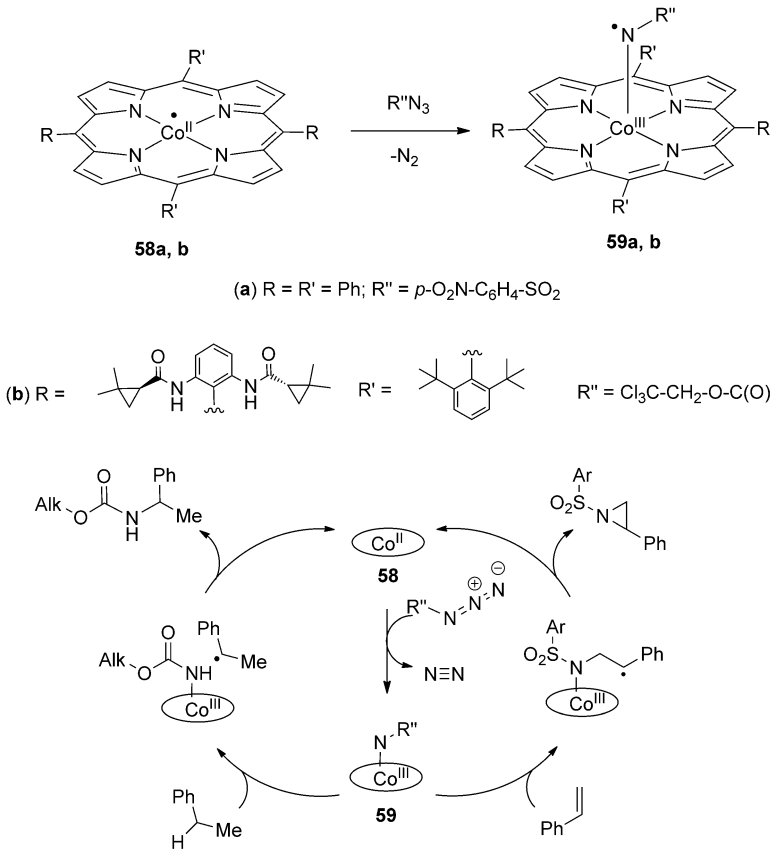

Scheme 22. Formation of Co^{III}-nitrene radical species **59** and their catalytic activity in C–H bond amination and olefin aziridination.[44]

bond-donor substituents, are much faster than those with (TPP)Co^{II} **58a**. Furthermore, faster formation of **59b** is observed in EPR studies. This is likely due to stabilization of nitrene radical **59b** as well as the transition state leading to its formation through hydrogen bonding of the nitrene radical ligand with the amide functionalities of the porphyrin ligand in the second coordination sphere of the complex (Figure 6).

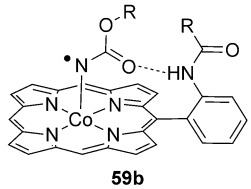

Figure 6. Hydrogen-bond donors in the second coordination sphere stabilizing the nitrene radical **59b** and accelerating its formation.

A related stabilizing effect by different Lewis acids was recently reported by Ray and co-workers for a Cu-nitrene-radical species.[46] Here, reaction of Cu^{I} complex **60** (Scheme 23) with a soluble iodosobenzene derivative ^{s}PhI=NTs immediately leads to formation of Cu^{II} complex **62**, presumably by abstraction of a hydrogen atom from the solvent (or traces of moisture) by "nitrene radical" intermediate **61**. Different Lewis acids were added to stabilize species **61** for further characterization and reactivity studies, with scandium(III) triflate proving the most efficient. The thus-stabilized "nitrene radical" species **61-Sc** is capable of oxidizing 2 equivalents of ferrocene to ferrocenium (yield of Fc^{+} is 180%), thus showing that **61-Sc** is two oxidation levels above the starting compound **60**. XAS measurements reveal that **61-Sc** is a Cu^{II} species (not Cu^{III}), based on the **61-Sc** pre-edge energy (ca. 8978 eV; almost identical to the pre-edge energy of the unambiguous Cu^{II} complex **62**). This allowed the authors to assign **61-Sc** as a Cu^{II}-nitrene-radical species. Complex **61-Sc** also participates in HAA (with dihydroantracene and 1,4-cyclohexadiene) to give **62** and the corresponding aromatic organic compounds. **61-Sc** is also active in nitrene C–H bond insertion reactions with toluene and cyclohexane, thereby yielding amine derivatives with a small amount of imines (Scheme 23). The stabilizing effect of Sc^{III} ions is most probably the result of the reduced electron density on the nitrene nitrogen atom of **61**, which also decreases its HAA reactivity.

Besides the discussed experimentally characterized nitrene-centered radical complexes, there are a number of additional mechanistic studies on transition-metal-catalyzed aziridination and amination reactions, where nitrene-centered radical ligands are proposed (or computationally found) to be key intermediates. These calculations mainly focused on Cu^{I}-,[47] Cu^{II}-, and Ag^{I}-catalyzed aziridination and nitrene insertion reactions.[48] Nitrene species derived from **40** as well as Fe and Co porphyrin species bearing nitrenes have also been studied computationally.[44,49] Redox-active NAr fragments might also be present in some Ni-NAr species related to **26** and **33**.[50]

4. Nitridyl Radical Complexes

From the above sections it is clear that nitrogen-centered aminyl- and nitrene-based radical ligands, although being less stable than their metalloradical imido and amido counterparts, can show selective reactivity, and remain "controlled" by the metal d orbitals. This concept is highly interesting from a synthetic point of view, and is (at least conceptually) worth considering in view of the activation of dinitrogen with open-shell transition-metal complexes. As such, the formation of nitridyl radical complexes ([M(•N)]) from N_2 can be expected (Figure 1c), possibly allowing subsequent reactivity with other (organic) substrates. This possibility has thus far been rarely investigated, but some recent examples reveal the potential.

In this context, the detection of an iridium nitridyl radical and its inherent radical-type reactivity, as recently reported by Schneider, de Bruin, and co-workers, is of particular interest. The synthesis of Ir^{II} azide complex **63** was disclosed, which

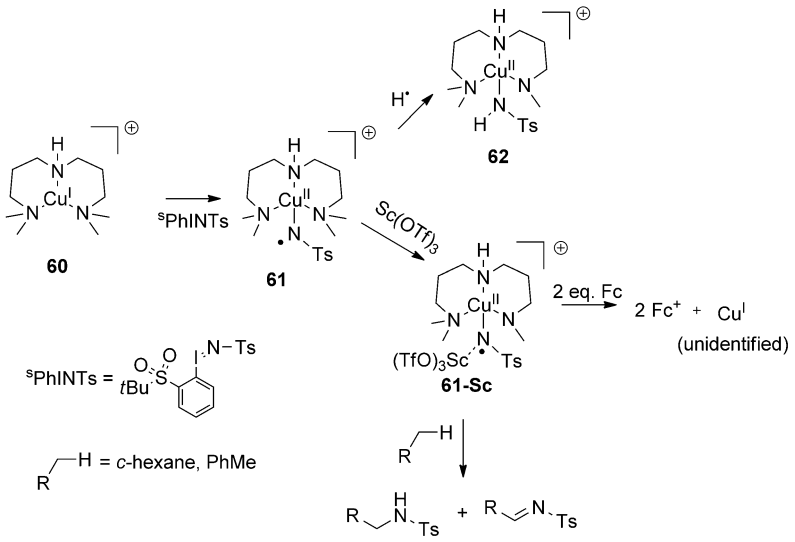

Scheme 23. Stabilizing effect of Sc^{III} ions, which slow down the HAA activity of Cu^{II}-nitrene radical species **61**.[46] Ts = toluene-4-sulfonyl, OTf = triflate.

character of this system so far precludes a definitive assignment or classification.

Compound **64** is stable at room temperature for several minutes, but then dimerizes to the dinuclear N_2-bridged Ir^I species **66**. This species reacts subsequently with nitrogen (probably formed during decomposition of **63**) to give the mononuclear Ir^I-N_2 complex **67** (Scheme 24). Complex **64** is not reactive towards C–H bonds 1,4-cyclohexadiene, and gives only **66** and **67**, which is probably due to the kinetic preference for dimerization over HAA.

Wieghardt and co-workers reported the synthesis of a related "nitridyl radical" species **69** (together with some related species), which was prepared by photolysis of the corresponding azide **68** (Scheme 25).[52] The authors interpreted complex **69** as predominantly a nitrido Fe^V species, but DFT calculations show that the SOMO of **69** has about 75% "nitridyl radical"

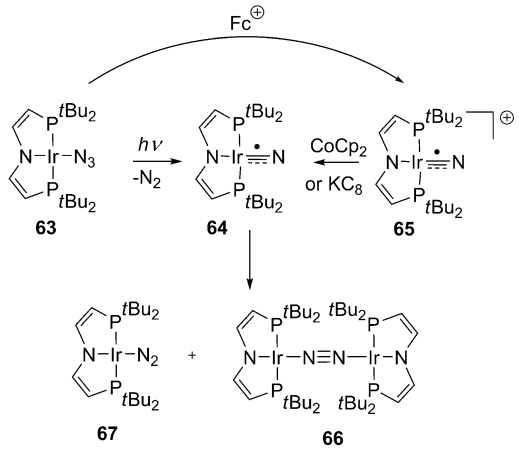

Scheme 24. Formation of Ir^{III}-nitridyl radical **64** and its radical-coupling reaction to form N_2-bridged binuclear Ir^I complex **66**.[51]

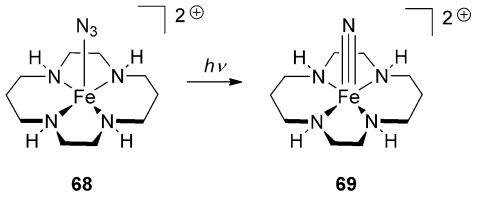

Scheme 25. Photolysis of azido complex **68** to **69**; iron(V) nitrido or iron(IV) nitridyl radical species?[52]

upon irradiation produces neutral iridium "nitridyl radical" complex **64** (Scheme 24).[51] Alternatively, species **64** can be generated by reduction of cationic nitrido complex **65**, which in turn is obtained by oxidation of **63** with a ferrocenium salt. The EPR (20 K) spectrum of **64** shows a rhombic signal with large *g*-anisotropy ($g_1 = 1.885$, $g_2 = 1.632$, $g_3 = 1.320$). Remarkably, all the *g*-values of **64** are below 2.0, which indicates that spin-orbit coupling interactions with empty d orbitals are strong, but negligible with filled d orbitals.

DFT calculations showed an almost covalent Ir–N bond with about 50% of the total spin density on the non-PNP nitrogen atom and 40% on the iridium atom, thus indicating a substantial contribution of the Ir-N$^{\bullet}$ nitridyl radical resonance structure. The unpaired electron is located in a π^* Ir-N molecular orbital, and hence this system can be described as a 1e-reduced Fischer-type species. The substantial covalent character. Hence, species **69** might also have been described as a nitridyl radical Fe^{IV} species.

The previously discussed nitrido (nitridyl) complexes were prepared from azido precursors. A recent example reported by Holland and co-workers[53] is especially noteworthy, since it was obtained by the stoichiometric activation of N_2 by an iron β-diketiminate complex (**70**). This led to the formation of the bridging bis(nitrido)iron cluster **71** (Scheme 26). The tetranuclear cluster is only formed in THF, and includes two potassium cations stemming from the reductant (KC_8). X-ray crystallographic studies of **71** reveal an N-N distance of 2.799(2) Å, consistent with the absence of any N–N bond. Based on Mössbauer spectroscopy and magnetic susceptibility measurements, Fe(1) and Fe(2) are both assigned as high-spin Fe^{III} centers, whereas Fe(3) and Fe(4) are high-spin Fe^{II} centers (Scheme 26). The calculations, performed on a simplified model, show quite a high contribution of the nitrogen-based atomic orbitals to the HOMO (exact numbers are not reported), which suggests that the unpaired electron is probably delocalized over the nitrido moieties and the Fe centers. A more detailed analysis of the electronic structure of **71** would be required to confirm this. Complex **71** is able to activate H_2 at room temperature, and affords ammonia in 42% yield. This reaction can currently only be performed in a stoichiometric fashion.

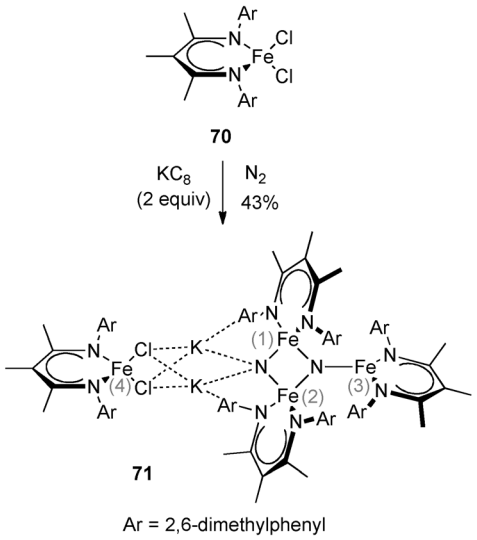

Scheme 26. Reductive activation of dinitrogen at Fe^{III} complex **70** leading to nitride-bridged cluster **71.**[53]

5. Conclusions

The detection and targeted synthesis of nitrogen-centered radical ligand complexes has attracted a lot of attention over the past decade. The relevance of these intriguing species lies in their reactivity, and several aminyl ([M(·NR_2)]) and nitrene/imido radical complexes ([M(·NR)]) are active intermediates in different catalytic and stoichiometric nitrogen transfer processes. These species often reveal selective radical-type reactivity, including addition to unsaturated bonds, radical–radical coupling, as well as hydrogen atom abstraction reactions. The full benefit of such radical-type reactivity becomes apparent when considering transformations of unactivated substrates such as alkanes, which lack donor atoms and are not prone to form anionic or cationic intermediates, but nonetheless can be successfully transformed through radical C–H functionalization pathways into amines by using aminyl or nitrene/imido radical complexes. The reactivity of the doublet radical ligand complexes described in this Review seems to correlate (qualitatively) with the amount of spin density located at the nitrogen atom. Moreover, a recent study by Pérez and co-workers reveals that spin-state transitions occur easily during nitrene transfer reactions, which might actually be more general.[47g] Hence radicaloid pathways involving excited-state triplets can even be expected for imido/nitrene species with a closed-shell ground state reacting via triplet- or singlet-biradical exited states.

Resolving the (electronic) structures of nitrogen-centered radical complexes is generally based on a number of spectroscopic techniques such as EPR, X-ray absorption, and Mössbauer spectroscopy as well as X-ray crystallography, often combined with DFT calculations. This allows a classification of these radical ligand species as 1e-reduced Fischer-type, 1e-oxidized Schrock-type or covalent systems. Most of the reported complexes represent either 1e-reduced Fischer-type systems or have rather covalent M–N bonds, while 1e-oxidized Schrock-species are rare. Although it is tempting to think that the 1e-oxidized Schrock-type systems may reveal quite different reactivity patterns from those reported for the 1e-reduced Fischer-type systems, at this point no comparative reactivity studies and too few examples describing (the reactivity of) 1e-oxidized Schrock-type systems are available to make any fair comparisons. Future investigations should shine more light on this matter, and hence we encourage scientists in this field to consider these aspects and to not report only the spin density of the calculated complexes with nitrogen-centered radical ligands but also the nature of metal–nitrogen π bond.

Among the family of aminyl, imidyl/nitrene radical, and nitridyl metal complexes, the last are remarkably rare. This is not unexpected in view of the low steric protection of the "naked" nitrogen atom in nitridyl species. However, despite clear difficulties in the synthesis and isolation of such nitridyl radical complexes, the role they might play in, for example, dinitrogen, fixation makes them valuable synthetic targets for future reactivity studies. Their potential reactivity towards other small molecules and organic substrates is also of particular interest.

This work was financially supported by the European Research Council (Grant Agreement 202886), The Netherlands Organization for Scientific Research (NWO-CW VICI grant 016.122.613) and the University of Amsterdam.

Received: February 20, 2013
Published online: November 8, 2013

[1] For reviews, see a) J. I. van der Vlugt, *Eur. J. Inorg. Chem.* **2012**, 363–375; b) J. I. van der Vlugt, J. N. H. Reek, *Angew. Chem.* **2009**, *121*, 8990–9004; *Angew. Chem. Int. Ed.* **2009**, *48*, 8832–8846. See also a special issue on "Cooperative & Redox Non-Innocent Ligands in Directing Organometallic Reactivity": *Eur. J. Inorg. Chem.* **2012**, *3*, 340–580, and references therein.

[2] For reviews, see a) V. Lyaskovskyy, B. de Bruin, *ACS Catal.* **2012**, *2*, 270–279; b) O. R. Luca, R. H. Crabtree, *Chem. Soc. Rev.* **2013**, *42*, 1440–1459; c) V. K. K. Praneeth, M. R. Ringenberg, T. R. Ward, *Angew. Chem.* **2012**, *124*, 10374–10380; *Angew. Chem. Int. Ed.* **2012**, *51*, 10228–10234; d) W. I. Dzik, J. I. van der Vlugt, J. N. H. Reek, B. de Bruin, *Angew. Chem.* **2011**, *123*, 3416–3418; *Angew. Chem. Int. Ed.* **2011**, *50*, 3356–3358; e) W. I. Dzik, X. P. Zhang, B. de Bruin, *Inorg. Chem.* **2011**, *50*, 9896–9903; f) B. de Bruin, D. G. H. Hetterscheid, *Eur. J. Inorg. Chem.* **2007**, 211–230; g) J. L. Boyer, J. Rochford, M.-K. Tsai, J. T. Muckerman, E. Fujita, *Coord. Chem. Rev.* **2010**, *254*, 309–330.

[3] For selected reviews, see a) W. Kaim, B. Schwederski, *Coord. Chem. Rev.* **2010**, *254*, 1580–1588; b) J. Stubbe, W. A. van der Donk, *Chem. Rev.* **1998**, *98*, 705–762; c) D. L. Harris, *Curr. Opin. Chem. Biol.* **2001**, *5*, 724–735; d) M. Sono, M. P. Roach, E. D. Coulter, J. H. Dawson, *Chem. Rev.* **1996**, *96*, 2841–2887.

[4] a) M. A. Bigi, S. A. Reed, M. C. White, *Nat. Chem.* **2011**, *3*, 218–224; b) H. Lu, V. Subbarayan, J. Tao, X. P. Zhang, *Organometallics* **2010**, *29*, 389–393; c) G.-Y. Gao, J. E. Jones, R. Vyas, J. D. Harden, X. P. Zhang, *J. Org. Chem.* **2006**, *71*, 6655–6658; d) V. Subbarayan, J. V. Ruppel, S. Zhu, J. A. Perman, X. P. Zhang, *Chem. Commun.* **2009**, 4266–4268.

[5] a) S. Itoh, M. Taki, S. Fukuzumi, *Coord. Chem. Rev.* **2000**, *198*, 3–20; b) P. Chaudhuri, K. Wieghardt, Prog. Inorg. Chem. **2002**,

50, 151 – 216; c) L. Mirica, X. Ottenwaelder, T. Stack, *Chem. Rev.* **2004**, *104*, 1013 – 1045; d) M. Costas, M. Mehn, M. Jensen, L. Que, *Chem. Rev.* **2004**, *104*, 939 – 986; e) C. Lyons, T. Stack, *Coord. Chem. Rev.* **2013**, *257*, 528 – 540.

[6] In some cases free organic aminyl radicals also show selective reactivity; for a review, see S. Z. Zard, *Chem. Soc. Rev.* **2008**, *37*, 1603 – 1618.

[7] Review: R. G. Hicks, *Angew. Chem.* **2008**, *120*, 7503 – 7505; *Angew. Chem. Int. Ed.* **2008**, *47*, 7393 – 7395.

[8] For iminobenzoquinonato radicals, see a) H. Chun, E. Bill, T. Weyhermüller, K. Wieghardt, *Inorg. Chem.* **2003**, *42*, 5612 – 5620; b) X. Sun, H. Chun, K. Hildenbrand, E. Bothe, T. Weyhermüller, F. Neese, K. Wieghardt, *Inorg. Chem.* **2002**, *41*, 4295 – 4303; c) K. Blackmore, M. Sly, M. Haneline, J. Ziller, A. Heyduk, *Inorg. Chem.* **2008**, *47*, 10522 – 10532; d) A. Nguyen, K. Blackmore, S. Carter, R. Zarkesh, A. Heyduk, *J. Am. Chem. Soc.* **2009**, *131*, 3307 – 3316; for verdazyl radical complexes, see e) S. McKinnon, B. Patrick, A. B. P. Lever, R. Hicks, *J. Am. Chem. Soc.* **2011**, *133*, 13587 – 13603; f) S. McKinnon, B. Patrick, A. B. P. Lever, R. Hicks, *Chem. Commun.* **2010**, *46*, 773 – 775; g) D. Brook, C. Richardson, B. Haller, M. Hundley, G. Yee, *Chem. Commun.* **2010**, *46*, 6590 – 6592; h) D. Brook, G. Yee, M. Hundley, D. Rogow, J. Wong, K. Van-Tu, *Inorg. Chem.* **2010**, *49*, 8573 – 8577; i) J.-B. Rota, L. Norel, C. Train, N. Amor, D. Maynau, V. Robert, *J. Am. Chem. Soc.* **2008**, *130*, 10380 – 10385.

[9] R. H. Crabtree, *The Organometallic Chemistry of the Transition Metals*, 5th ed., Wiley, Hoboken, **2009**.

[10] B. de Bruin, D. G. H. Hetterscheid, A. J. J. Koekkoek, H. Grützmacher, *Prog. Inorg. Chem.* **2007**, *55*, 247 – 354.

[11] A series of Mn^{I} complexes were classified as ligand-centered species: a) D. Sellmann, J. Müller, P. Hofmann, *Angew. Chem.* **1982**, *94*, 708 – 709; *Angew. Chem. Int. Ed. Engl.* **1982**, *21*, 691 – 692; b) D. Sellmann, J. Müller, *J. Organomet. Chem.* **1985**, *281*, 249 – 262; however, later those complexes were found to be best described as Mn^{II} amide species, based on EPR and UV/Vis measurements: c) R. Gross, W. Kaim, *Angew. Chem.* **1985**, *97*, 869 – 870; *Angew. Chem. Int. Ed. Engl.* **1985**, *24*, 856 – 858; d) R. Gross, W. Kaim, *Inorg. Chem.* **1987**, *26*, 3596 – 3600.

[12] a) F. N. Penkert, T. Weyhermüller, E. Bill, P. Hildebrandt, S. Lecomte, K. Wieghardt, *J. Am. Chem. Soc.* **2000**, *122*, 9663 – 9673; b) O. Schlager, K. Wieghardt, B. Nuber, *Inorg. Chem.* **1995**, *34*, 6456 – 6462.

[13] T. Büttner, J. Geier, G. Frison, J. Harmer, C. Calle, A. Schweiger, H. Schönberg, H. Grützmacher, *Science* **2005**, *307*, 235 – 238.

[14] S. Frantz, R. Reinhardt, S. Greulich, M. Wanner, J. Fiedler, C. Duboc-Toia, W. Kaim, *Dalton Trans.* **2003**, 3370 – 3375.

[15] N. Donati, D. Stein, T. Büttner, H. Schönberg, J. Harmer, S. Anadaram, H. Grützmacher, *Eur. J. Inorg. Chem.* **2008**, 4691 – 4703.

[16] a) P. Maire, M. Königsmann, A. Sreekanth, J. Harmer, A. Schweiger, H. Grützmacher, *J. Am. Chem. Soc.* **2006**, *128*, 6578 – 6580; b) N. Donati, M. Königsmann, D. Stein, L. Udino, H. Grützmacher, *C. R. Chim.* **2007**, *10*, 721 – 730; c) M. Königsmann, N. Donati, D. Stein, H. Schönberg, J. Harmer, A. Sreekanth, H. Grützmacher, *Angew. Chem.* **2007**, *119*, 3637 – 3640; *Angew. Chem. Int. Ed.* **2007**, *46*, 3567 – 3570.

[17] J. W. Whittaker, *Chem. Rev.* **2003**, *103*, 2347 – 2364.

[18] a) D. Morales-Morales, C. M. Jensen, *The Chemistry of Pincer Compounds*, Elsevier, Amsterdam, **2007**; b) G. van Koten, D. Milstein, *Organometallic Pincer Chemistry*, Springer, Dordrecht, **2012**; c) J. I. van der Vlugt, *Angew. Chem.* **2010**, *122*, 260 – 263; *Angew. Chem. Int. Ed.* **2010**, *49*, 252 – 255.

[19] D. Adhikari, S. Mossin, F. Basuli, J. C. Huffman, R. K. Szilagyi, K. Meyer, D. J. Mindiola, *J. Am. Chem. Soc.* **2008**, *130*, 3676 – 368.

[20] A. T. Radosevich, J. G. Melnick, S. A. Stoian, D. Bacciu, C.-H. Chen, B. M. Foxman, O. V. Ozerov, D. G. Nocera, *Inorg. Chem.* **2009**, *48*, 9214 – 9221.

[21] S. B. Harkins, N. P. Mankad, A. J. M. Miller, R. K. Szilagyi, J. C. Peters, *J. Am. Chem. Soc.* **2008**, *130*, 3478 – 3485.

[22] N. P. Mankad, W. E. Antholine, R. K. Szilagyi, J. C. Peters, *J. Am. Chem. Soc.* **2009**, *131*, 3878 – 3880.

[23] M. M. Melzer, S. Mossin, X. Dai, A. M. Bartell, P. Kapoor, K. Meyer, T. H. Warren, *Angew. Chem.* **2010**, *122*, 916 – 919; *Angew. Chem. Int. Ed.* **2010**, *49*, 904 – 907.

[24] S. Wiese, Y. M. Badiei, R. T. Gephart, S. Mossin, M. S. Varonka, M. M. Melzer, K. Meyer, T. R. Cundari, T. H. Warren, *Angew. Chem.* **2010**, *122*, 9034 – 9039; *Angew. Chem. Int. Ed.* **2010**, *49*, 8850 – 8855.

[25] R. T. Gephart III, D. L. Huang, M. J. B. Aguila, G. Schmidt, A. Shahu, T. H. Warren, *Angew. Chem.* **2012**, *124*, 6594 – 6598; *Angew. Chem. Int. Ed.* **2012**, *51*, 6488 – 6492.

[26] E. Kogut, H. L. Wiencko, L. Zhang, D. E. Cordeau, T. H. Warren, *J. Am. Chem. Soc.* **2005**, *127*, 11248 – 11249.

[27] S. Wiese, J. L. McAfee, D. R. Pahls, C. L. McMullin, T. R. Cundari, T. H. Warren, *J. Am. Chem. Soc.* **2012**, *134*, 10114 – 10121.

[28] a) D. J. Mindiola, G. L. Hillhouse, *Chem. Commun.* **2002**, 1840 – 1841; b) R. Waterman, G. L. Hillhouse, *J. Am. Chem. Soc.* **2008**, *130*, 12628 – 12629.

[29] V. M. Iluc, A. J. M. Miller, J. S. Anderson, M. J. Monreal, M. P. Mehn, G. L. Hillhouse, *J. Am. Chem. Soc.* **2011**, *133*, 13055 – 13063.

[30] Y. Miyazato, T. Wada, J. T. Muckerman, E. Fujita, K. Tanaka, *Angew. Chem.* **2007**, *119*, 5830 – 5832; *Angew. Chem. Int. Ed.* **2007**, *46*, 5728 – 5730.

[31] C. C. Lu, S. DeBeer George, T. Weyhermüller, E. Bill, E. Bothe, K. Wieghardt, *Angew. Chem.* **2008**, *120*, 6484 – 6487; *Angew. Chem. Int. Ed.* **2008**, *47*, 6384 – 6387.

[32] a) T. A. Betley, J. C. Peters, *J. Am. Chem. Soc.* **2003**, *125*, 10782 – 10783; b) C. M. Thomas, N. P. Mankad, J. C. Peters, *J. Am. Chem. Soc.* **2006**, *128*, 4956 – 4957.

[33] I. Nieto, F. Ding, R. P. Bontchev, H. Wang, J. M. Smith, *J. Am. Chem. Soc.* **2008**, *130*, 2716 – 2717.

[34] A. Takaoka, L. C. H. Gerber, J. C. Peters, *Angew. Chem.* **2010**, *122*, 4182 – 4185; *Angew. Chem. Int. Ed.* **2010**, *49*, 4088 – 4091.

[35] A. Takaoka, M. E. Moret, J. C. Peters, *J. Am. Chem. Soc.* **2012**, *134*, 6695 – 6706.

[36] N. P. Mankad, P. Müller, J. C. Peters, *J. Am. Chem. Soc.* **2010**, *132*, 4083 – 4085.

[37] E. R. King, E. T. Hennessy, T. A. Betley, *J. Am. Chem. Soc.* **2011**, *133*, 4917 – 4923.

[38] E. R. King, G. T. Sazama, T. A. Betley, *J. Am. Chem. Soc.* **2012**, *134*, 17858 – 17861.

[39] S. C. Bart, E. Lobkovsky, E. Bill, P. J. Chirik, *J. Am. Chem. Soc.* **2006**, *128*, 5302 – 5303.

[40] A. C. Bowman, C. Milsmann, E. Bill, Z. R. Turner, E. Lobkovsky, S. DeBeer, K. Wieghardt, P. J. Chirik, *J. Am. Chem. Soc.* **2011**, *133*, 17353 – 17369.

[41] See, for example: J. N. Harvey, *Struct. Bonding (Berlin)* **2004**, *112*, 151 – 184.

[42] a) N. A. Eckert, S. Vaddadi, S. Stoian, R. J. Lachicotte, T. R. Cundari, P. L. Holland, *Angew. Chem.* **2006**, *118*, 7022 – 7025; *Angew. Chem. Int. Ed.* **2006**, *45*, 6868 – 6871; b) R. E. Cowley, N. A. Eckert, S. Vaddadi, T. M. Figg, T. R. Cundari, P. L. Holland, *J. Am. Chem. Soc.* **2011**, *133*, 9796 – 9811; c) R. E. Cowley, N. J. DeYonker, N. A. Eckert, T. R. Cundari, S. DeBeer, E. Bill, X. Ottenwaelder, C. Flaschenriem, P. L. Holland, *Inorg. Chem.* **2010**, *49*, 6172 – 6187; d) P. L. Holland, *Acc. Chem. Res.* **2008**, *41*, 905 – 914.

[43] R. E. Cowley, P. L. Holland, *Inorg. Chem.* **2012**, *51*, 8352 – 8361.

[44] a) V. Lyaskovskyy, A. I. Olivos Suarez, H. Lu, H. Jiang, X. P. Zhang, B. de Bruin, *J. Am. Chem. Soc.* **2011**, *133*, 12264 – 12273; b) A. I. Olivos Suarez, H. Jiang, X. P. Zhang, B. de Bruin, *Dalton Trans.* **2011**, *40*, 5697 – 5705.

[45] a) J. D. Harden, J. V. Ruppel, G.-Y. Gao, X. P. Zhang, *Chem. Commun.* **2007**, 4644 – 4646; b) H. Lu, H. Jiang, L. Wojtas, X. P. Zhang, *Angew. Chem.* **2010**, *122*, 10390 – 10394; *Angew. Chem. Int. Ed.* **2010**, *49*, 10192 – 10196; c) H. Lu, J. Tao, J. E. Jones, L. Wojtas, X. P. Zhang, *Org. Lett.* **2010**, *12*, 1248 – 1251; d) J. V. Ruppel, R. M. Kamble, X. P. Zhang, *Org. Lett.* **2007**, *9*, 4889 – 4892.

[46] S. Kundu, E. Miceli, E. R. Farquhar, F. F. Pfaff, U. Kuhlmann, P. Hildebrandt, B. Braun, C. Greco, K. Ray, *J. Am. Chem. Soc.* **2012**, *134*, 14710 – 14713.

[47] a) M. M. Díaz-Requejo, P. J. Pérez, M. Brookhart, J. L. Templeton, *Organometallics* **1997**, *16*, 4399 – 4402; b) P. Brandt, M. J. Södergren, P. G. Andersson, P.-O. Norrby, *J. Am. Chem. Soc.* **2000**, *122*, 8013 – 8020; c) D. N. Barman, P. Liu, K. N. Houk, K. M. Nicholas, *Organometallics* **2010**, *29*, 3404 – 3412; d) T. R. Cundari, A. Dinescu, A. B. Kazi, *Inorg. Chem.* **2008**, *47*, 10067 – 10072; e) Y. M. Badiei, A. Dinescu, X. Dai, R. M. Palomino, F. W. Heinemann, T. R. Cundari, T. H. Warren, *Angew. Chem.* **2008**, *120*, 10109 – 10112; *Angew. Chem. Int. Ed.* **2008**, *47*, 9961 – 9964; f) S. M. Tekarli, T. G. Williams, T. R. Cundari, *J. Chem. Theory Comput.* **2009**, *5*, 2959 – 2966; g) L. Maestre, W. M. C. Sameera, M. M. Díaz-Requejo, F. Maseras, P. J. Pérez, *J. Am. Chem. Soc.* **2013**, *135*, 1338 – 1348.

[48] a) P. Comba, C. Haaf, A. Lienke, A. Muruganantham, H. Wadepohl, *Chem. Eur. J.* **2009**, *15*, 10880 – 10887; b) F. Mohr, S. A. Binfield, J. C. Fettinger, A. N. Vedernikov, *J. Org. Chem.* **2005**, *70*, 4833 – 4839.

[49] a) E. Tangen, J. Conradie, A. Ghosh, *J. Chem. Theory Comput.* **2007**, *3*, 448 – 457; b) K. H. Hopmann, A. Ghosh, *ACS Catal.* **2011**, *1*, 597 – 600.

[50] a) G. Bai, D. W. Stephan, *Angew. Chem.* **2007**, *119*, 1888 – 1891; *Angew. Chem. Int. Ed.* **2007**, *46*, 1856 – 1859; b) T. R. Cundari, J. O. Jimenez-Halla, G. R. Morello, S. Vaddadi, *J. Am. Chem. Soc.* **2008**, *130*, 13051 – 13058.

[51] M. G. Scheibel, B. Askevold, F. W. Heinemann, E. J. Reijerse, B. de Bruin, S. Schneider, *Nature Chem.* **2012**, *4*, 552 – 558.

[52] a) K. Meyer, E. Bill, B. Mienert, T. Weyhermuller, K. Wieghardt, *J. Am. Chem. Soc.* **1999**, *121*, 4859 – 4876; b) C. A. Grapperhaus, B. Mienert, E. Bill, T. Weyhermuller, K. Wieghardt, *Inorg. Chem.* **2000**, *39*, 5306 – 5317; c) N. Aliaga-Alcalde, S. DeBeer George, B. Mienert, E. Bill, K. Wieghardt, F. Neese, *Angew. Chem.* **2005**, *117*, 2968 – 2972; *Angew. Chem. Int. Ed.* **2005**, *44*, 2908 – 2912; d) J. F. Berry, E. Bill, E. Bothe, S. DeBeer George, B. Mienert, F. Neese, K. Wieghardt, *Science* **2006**, *312*, 1937 – 1941.

[53] a) M. M. Rodriguez, E. Bill, W. W. Brennessel, P. L. Holland, *Science* **2011**, *334*, 780 – 783; b) T. M. Figg, P. L. Holland, T. R. Cundari, *Inorg. Chem.* **2012**, *51*, 7546 – 7550.

